A peer-reviewed version of this preprint was published in PeerJ on 21 February 2019.

View the peer-reviewed version (peerj.com/articles/6432), which is the preferred citable publication unless you specifically need to cite this preprint.

Snively E, O'Brien H, Henderson DM, Mallison H, Surring LA, Burns ME, Holtz TR Jr, Russell AP, Witmer LM, Currie PJ, Hartman SA, Cotton JR. 2019. Lower rotational inertia and larger leg muscles indicate more rapid turns in tyrannosaurids than in other large theropods. PeerJ 7:e6432 https://doi.org/10.7717/peerj.6432

PeerJ Preprints NOT PEER-REVIEWED

Lower rotational inertia and larger leg muscles indicate more rapid turns in tyrannosaurids than in other large theropods

Eric Snively [Corresp., 1] , **Haley O'Brien** [2] , **Donald M Henderson** [3] , **Heinrich Mallison** [4] , **Lara A Surring** [3] , **Michael E Burns** [5] , **Thomas R Holtz, Jr.** [6,7] , **Anthony P Russell** [8] , **Lawrence M Witmer** [9] , **Philip J Currie** [10] , **Scott A Hartman** [11] , **John R Cotton** [12]

[1] Department of Biology, University of Wisconsin-La Crosse, United States
[2] Department of Anatomy and Cell Biology, Oklahoma State University College of Osteopathic Medicine, Tulsa, Oklahoma, United States
[3] Royal Tyrrell Museum of Palaeontology, Drumheller, Alberta, Canada
[4] Museum fur Naturkunde, Berlin, Germany
[5] Department of Biology, Jacksonville State University, Jacksonville, Alabama, United States
[6] Department of Geology, University of Maryland, College Park, Maryland, United States
[7] Department of Paleobiology, National Museum of Natural History, Washington, D.C., United States
[8] Department of Biological Sciences, University of Calgary, Calgary, Alberta, Canada
[9] Department of Biomedical Sciences, Ohio University, Athens, Ohio, United States
[10] Department of Biological Sciences, University of Alberta, Edmonton, Albeta, Canada
[11] Department of Geoscience, University of Wisconsin-Madison, Madison, WI, United States
[12] Department of Mechanical Engineering, Ohio University, Athens, Ohio, United States

Corresponding Author: Eric Snively
Email address: esnively@uwlax.edu

Synopsis: Tyrannosaurid dinosaurs had larger than predicted preserved leg muscle attachments and low rotational inertia relative to their body mass, indicating that they could turn more quickly than other large theropods. **Methods:** To compare turning capability in theropods, we regressed agility estimates against body mass, incorporating superellipse-based modeled mass, centers of mass, and rotational inertia (mass moment of inertia). Muscle force relative to body mass is a direct correlate of agility in humans, and torque gives potential angular acceleration. Agility scores therefore include rotational inertia values divided by proxies for (1) muscle force (ilium area and estimates of m. caudofemoralis longus cross-section), and (2) musculoskeletal torque. Phylogenetic ANCOVA (phylANCOVA) allow assessment of differences in agility between tyrannosaurids and non-tyrannosaurid theropods (accounting for both ontogeny and phylogeny). We applied conditional error probabilities *a(p)* to stringently test the null hypothesis of equal agility. **Results:** Tyrannosaurids consistently have agility index magnitudes twice those of allosauroids and some other theropods of equivalent mass, turning the body with both legs planted or pivoting over a stance leg. PhylANCOVA demonstrates definitively greater agilities in tyrannosaurids, and phylogeny explains nearly all covariance. Mass property results are consistent with those of other studies based on skeletal mounts, and between different figure-based methods (our main mathematical slicing procedures, lofted 3D

PeerJ Preprints NOT PEER-REVIEWED

computer models, and simplified graphical double integration). **Implications:** The capacity for relatively rapid turns in tyrannosaurids is ecologically intriguing in light of their monopolization of large (>400 kg), toothed dinosaurian predator niches in their habitats.

PeerJ Preprints NOT PEER-REVIEWED

Title

Lower rotational inertia and larger leg muscles indicate more rapid turns in tyrannosaurids than in other large theropods

Authors

Eric Snively[1], Haley O'Brien[2], Donald M. Henderson[3], Heinrich Mallison[4], Lara A. Surring[3], Michael E. Burns[5], Thomas R. Holtz Jr.[6,7], Anthony P. Russell[8], Lawrence M. Witmer[9], Philip J. Currie[10], Scott A. Hartman[11], John R. Cotton[12]

Affiliations

[1]Deptartment of Biology, University of Wisconsin-La Crosse, La Crosse, WI, USA
[2]Department of Anatomy and Cell Biology, Oklahoma State University, Tulsa, OK, USA
[3]Royal Tyrrell Museum of Palaeontology, Drumheller, AB, Canada
[4] Museum für Naturkunde Berlin, Berlin, Germany
[5]Department of Biology, Jacksonville State University, Jacksonville, AB, USA
[6]Department of Geology, University of Maryland, College Park, MD, USA
[7]Department of Paleobiology, National Museum of Natural History, Washington, DC, USA
[8]Department of Biological Sciences, University of Calgary, Calgary, AB, Canada
[9]Department of Biomedical Sciences, Ohio University, Athens, OH, USA
[10]Department of Biological Sciences, University of Alberta, Edmonton, AB, Canada
[11]Department of Geoscience, University of Wisconsin, Madison, WI, USA
[12]Department of Mechanical Engineering, Russ College of Engineering and Technology, Ohio University, Athens, OH, USA

Corresponding Author
Eric Snively
Dept. of Biology
University of Wisconsin-La Crosse
1725 State Street
La Crosse, WI 54601

PeerJ Preprints | https://doi.org/10.7287/peerj.preprints.27021v1 | CC BY 4.0 Open Access | rec: 4 Jul 2018, publ: 4 Jul 2018

PeerJ Preprints NOT PEER-REVIEWED

Abstract

Synopsis: Tyrannosaurid dinosaurs had large preserved leg muscle attachments and low rotational inertia relative to their body mass, indicating that they could turn more quickly than other large theropods. **Methods:** To compare turning capability in theropods, we regressed agility estimates against body mass, incorporating superellipse-based modeled mass, centers of mass, and rotational inertia (mass moment of inertia). Muscle force relative to body mass is a direct correlate of agility in humans, and torque gives potential angular acceleration. Agility scores therefore include rotational inertia values divided by proxies for (1) muscle force (ilium area and estimates of m. caudofemoralis longus cross-section), and (2) musculoskeletal torque. Phylogenetic ANCOVA (phylANCOVA) allow assessment of differences in agility between tyrannosaurids and non-tyrannosaurid theropods (accounting for both ontogeny and phylogeny). We applied conditional error probabilities $\alpha(p)$ to stringently test the null hypothesis of equal agility. **Results:** Tyrannosaurids consistently have agility index magnitudes twice those of allosauroids and some other theropods of equivalent mass, turning the body with both legs planted or pivoting over a stance leg. PhylANCOVA demonstrates definitively greater agilities in tyrannosaurids, and phylogeny explains nearly all covariance. Mass property results are consistent with those of other studies based on skeletal mounts, and between different figure-based methods (our main mathematical slicing procedures, lofted 3D computer models, and simplified graphical double integration). **Implications:** The capacity for relatively rapid turns in tyrannosaurids is ecologically intriguing in light of their monopolization of large (>400 kg), toothed dinosaurian predator niches in their habitats.

PeerJ Preprints | https://doi.org/10.7287/peerj.preprints.27021v1 | CC BY 4.0 Open Access | rec: 4 Jul 2018, publ: 4 Jul 2018

Introduction

Tyrannosaurid theropods were ecologically unusual dinosaurs (Brusatte et al. 2010), and were as adults the only toothed terrestrial carnivores larger than 60 kg (Farlow and Holtz 2002) across much of the northern continents in the late Cretaceous. They ranged in adult trophic morphology from slender-snouted animals such as *Qianzhousaurus sinensis* (Li et al. 2009, Lü et al. 2014) to giant bone-crushers including *Tyrannosaurus rex* (Rayfield 2004, Hurum and Sabath 2003, Snively et al. 2006, Brusatte et al. 2010, Hone et al. 2011, Bates and Falkingham 2012, Gignac and Erickson 2017). In addition to the derived features of their feeding apparatus, the arctometatarsalian foot of tyrannosaurids likely contributed to effective prey capture through rapid linear locomotion and enhanced capability of the foot to resist torsion when maneuvering (Holtz 1995, Snively and Russell 2003, Surring et al., in revision). Features suggestive of enhanced agility (rate of turn) and tight maneuverability (radius of turn) in tyrannosaurids include relatively short bodies from nose to tail (anteroposteriorly short thoracic regions, and cervical vertebrae that aligned into posterodorsally retracted necks), small forelimbs, and long, tall ilia for leg muscle attachment (Paul 1988, Henderson and Snively 2003, Bakker and Bir 2004, Hutchinson et al. 2011). Here we present a biomechanical model that suggests tyrannosaurids could turn with greater agility, thus pivoting more quickly, than other large theropods, suggesting enhanced ability to pursue and subdue prey.

Like other terrestrial animals, large theropods would turn by applying torques (cross products of muscle forces and moment arms) to impart angular acceleration to their bodies. This angular acceleration can be calculated as musculoskeletal torque divided by the body's mass moment of inertia (=rotational inertia). Terrestrial vertebrates such as cheetahs can induce a tight turn by lateroflexing and twisting one part of their axial skeleton, such as the tail, and then

PeerJ Preprints | https://doi.org/10.7287/peerj.preprints.27021v1 | CC BY 4.0 Open Access | rec: 4 Jul 2018, publ: 4 Jul 2018

rapidly counterbending with the remainder, which pivots and tilts the body (Wilson et al. 2013, Patel and Braae 2014, Patel et al. 2016). The limbs can then accelerate the body in a new direction (Wilson et al. 2013). These tetrapods can also cause a larger-radius turn by accelerating the body more quickly with one leg than the other (pushing off with more force on the outside of a turn), which can incorporate hip and knee extensor muscles originating from the ilium and tail (Table 1). Hence muscles originating from the ilium can cause yaw (lateral pivoting) of the entire body, although they do not induce yaw directly. Such turning balances magnitudes of velocity and lean angle, and centripetal and centrifugal limb-ground forces. When limbs are planted on the ground, the body can pivot with locomotor muscle alone. In either case, limb muscles actuate and stabilize their joints, positively accelerating and braking the body and limbs.

Forces from locomotor muscles have a fundamental influence on agility. Torques from these limb muscles are necessary for estimating absolute angular acceleration (Hutchinson et al. 2007), and muscle power also influences turning rate (Young et al. 2002). However, experimental trials with human athletes show that agility scales directly with maximal muscle force, relative to body mass (Peterson et al. 2006, Thomas et al. 2009, Weiss et al. 2010). Relative (not absolute) maximal muscle force is straightforward to estimate directly and consistently from fossil evidence, compared to musculoskeletal moment arms that vary continuously with posture in three dimensions, or physiologically variable factors such as muscle power (Young et al. 2002). Muscle force is therefore a useful, replicable metric for comparative assessments of agility in fossil tetrapods. Estimates of theropod muscle force and the mass properties of their bodies can facilitate comparisons of turning ability in theropods of similar body mass.

PeerJ Preprints | https://doi.org/10.7287/peerj.preprints.27021v1 | CC BY 4.0 Open Access | rec: 4 Jul 2018, publ: 4 Jul 2018

This relative agility in theropods is testable by regressing estimated body mass (Fig. 1) against indicators of agility, which incorporate fossil-based estimates of muscle force (Fig. 2), torque, and body mass and mass moment of inertia (MMI; Fig. 1). Given the same moment arm lengths, greater force relative to rotational inertia indicates the ability to turn more rapidly. Coupled with protracted juvenile growth periods (Erickson et al. 2004), heightened agility would be consistent with the hypothesis that tyrannosaurids were predominantly predatory, and help to explain how late Campanian and Maastrichtian tyrannosaurids monopolized the large predator niche in the Northern Hemisphere.

Estimating mass properties and comparative turning performance of carnivorous dinosaurs

To compare agility in theropods, we divided ilium area (a proxy for muscle cross sectional area and maximal force production), and estimated m. caudofemoralis longus cross-sections, by I_y (rotational inertia in yaw about the body's center of mass). We also incorporated scaling of moment arm size in a separate analysis to better compare absolute turning performance in the theropods. We restrict our comparisons to proxies of agility at given body masses, rather than estimating absolute performance, because a generalized predictive approach enables us to compare many taxa. Viable paths for testing our results include musculoskeletal dynamics of turning involving all hind limb muscles, as undertaken by Rankin et al. (2016) for linear locomotion in ostriches, or simpler approaches such as Hutchinson et al.'s (2007) calculations for turning in *Tyrannosaurus*. However, the dynamics of turning are complicated to pursue even in extant dinosaurs (Jindrich et al. 2007), and estimating absolute performance in multiple extinct taxa would entail escalating numbers of assumptions with minimal comparative return. We therefore focus here on relative metrics of turning performance, based as much as possible on direct fossil data.

PeerJ Preprints | https://doi.org/10.7287/peerj.preprints.27021v1 | CC BY 4.0 Open Access | rec: 4 Jul 2018, publ: 4 Jul 2018

125 Using relative indices of agility, encompassing origins for relevant ilium-based muscles,
126 tail-originating muscles (Table 1), and mass moments of inertia, enables us to address action
127 beyond yaw alone. Muscles of the leg on the outside of a turn normally involved in linear
128 motion would change the body's direction by linearly accelerating the body in that direction,
129 while muscles for the leg on the inside of the turn exert less torque. Muscles involved in
130 stabilizing the limbs and body, and providing contralateral braking and abduction, would come
131 into play during rotation of the body. Mass moment of inertia is the most stringent mass-property
132 limit on turning ability in long, massive dinosaurs (Carrier et al. 2001, Henderson and Snively
133 2003). This simplified approach is predictive, testable with more complex investigations
134 (including specific torques of muscle-bone couples: Hutchinson et al. 2007), and allows broad
135 comparisons of overall turning ability.
136 Our hypotheses of comparative agility in large theropods incorporate two behavioral
137 scenarios potentially important for prey capture.
138 Hypothesis 1: Tyrannosaurids could turn their bodies more quickly than other theropods when
139 close to prey, pivoting the body with both feet planted on the ground.
140 Hypothesis 2. Tyrannosaurids could turn more quickly than other theropods when approaching
141 prey, pivoting the body plus a suspended swing leg above one stance foot planted on the ground.
142 Under the scenario in Hypothesis 1, the applicable mass moment of inertia I_y is that of the
143 body not including the hind legs, about a vertical axis through the body's center of mass.
144 Intuitively the body would yaw about a vertical line between the acetabula, but the centers of
145 mass of bipedal dinosaurs, and therefore their feet and ground reaction forces in this stance, are
146 almost always estimated to be anterior to the acetabulum (Henderson 1999, Hutchinson et al.

PeerJ Preprints | https://doi.org/10.7287/peerj.preprints.27021v1 | CC BY 4.0 Open Access | rec: 4 Jul 2018, publ: 4 Jul 2018

2007, Allen et al. 2009, Bates et al. 2009a, b; Hutchinson et al. 2011, Bates et al. 2012, Allen et al. 2013).

In a prey pursuit scenario under Hypothesis 2, the theropod has just pushed off with its swing leg, and is pivoting about its stance leg as it protracts the swing leg. The body and swing leg are rotating about their collective center of mass (COM), directly above the stance foot. Total I_y in this case includes the entire axial body (minus the hind legs), and the contribution of the swing leg to total I_y of the system.

Materials and methods

Comparing relative turning performance in tyrannosaurids and other theropods requires data on mass moment of inertia (MMI) I_y about a vertical axis (y) through the body's center of mass (COM), and estimates of leg muscle force and moment arms. (We sometimes use the abbreviation MMI rather than I to refer to mass moment of inertia because I is also the symbol for area moment of inertia.) To estimate mass, COM, and MMI, we approximated the bodies of the theropods as connected frusta (truncated cones or pyramids) with superellipse cross-sections (Fig. 1). Superellipses are symmetrical shapes the outline of which (from star-shaped, to ellipse, to rounded rectangle) are governed by exponents and major and minor dimensions (Rosin 2000, Motani 2001, Snively et al. 2013).

Spreadsheet templates for calculations of dimensions, mass, centers of mass, and rotational inertias are available as supplementary information. These enable the estimation of mass properties from cross-sectional and length dimensions, using Microsoft Excel-compatible software. Snively et al. (2013) provide coefficients and polynomial regression equations for super-elliptical frusta.

PeerJ Preprints | https://doi.org/10.7287/peerj.preprints.27021v1 | CC BY 4.0 Open Access | rec: 4 Jul 2018, publ: 4 Jul 2018

Specimens

Theropod specimens (Table 2) were included if they had complete ilia, and relatively complete skeletons ideally including the tail. If tails were incomplete they were reconstructed from other specimens of the same or a closely related genus, following the practice of Taylor (2009). Tyrannosaurid adults and juveniles are well represented by complete skeletons. Most other taxa were allosauroids, many of which are known from complete or rigorously reconstructable skeletons. *Yangchuanosaurus shangyouensis* and *Sinraptor hepingensis* are basal allosauroids. Their relative *Sinraptor dongi* lacks a preserved tail, and the older *Monolophosaurus jiangi* has a complete axial skeleton but lacks preserved hind legs, which are necessary for reliable mass estimates. Both species were therefore omitted. An early relative of allosauroids and tyrannosaurs, *Eustreptospondylus oxoniensis*, was included as a nearly complete, small representative of an allosauroid body plan, because it has a similar ratio of ilium/femur length as a less-complete juvenile specimen of *Allosaurus fragilis* (Foster and Chure 2006), and is a reasonable proxy for the basal allosauroid condition. The non-tetanuran theropods *Dilophosaurus wetherelli* and *Ceratosaurus nasicornis* were included for their similarity in size to juvenile tyrannsaurids, and to enable examination of how phylogeny affects patterns of mass moment of inertia versus muscle force. We include the small tyrannosaur that Sereno et al. (2009) named *Raptorex kriegsteini*. Fowler et al. (2011) provide evidence that this specimen is a juvenile *Tarbosaurus bataar* (see also Brusatte and Carr 2016). We informally refer to it as *Raptorex* to differentiate it from a much larger juvenile *Tarbosaurus* in our sample.

Digitizing of body outlines

Technical skeletal reconstructions by Paul (1988, 2010) and Hartman (2011), in dorsal and lateral views, were scanned on a flatbed scanner or saved as images (Hartman 2011),

PeerJ Preprints | https://doi.org/10.7287/peerj.preprints.27021v1 | CC BY 4.0 Open Access | rec: 4 Jul 2018, publ: 4 Jul 2018

vectorized with the Trace function in Adobe illustrator, and "expanded" for editing the entire outlines and individual bones. Lateral and dorsal outlines were modified based on body dimensions such as trunk, neck, and head length, and trunk and tail depth, as measured from scaled figures in the primary literature (Osborn 1917; Gilmore 1920; Russell 1970; Dong 1983; Gao 1992; Brochu 2003; Bates 2009a, b) and photographs of skeletons. We modified these outlines with updated anatomical data on neck and tail dimensions (Snively and Russell 2007a, Allen et al. 2009, Persons and Currie 2010), and the jaws were positioned as closed. The chevrons of *Giganotosaurus* were angled posteroventrally to match those of its relatives *Acrocanthosaurus* and *Allosaurus*. Dorsal and lateral views were scaled to the same length, and divided into 60+ segments with lines crossing corresponding structures in both views (Fig. 1). Coordinates were digitized for dorsal, ventral, midsagittal, and lateral contours using PlotDigitizer (Huwaldt 2010), scaled to femur lengths of the specimens. Coordinates were opened as CSV data in Microsoft Excel.

If a dorsal reconstruction of the skeleton was unavailable, a dorsal view of the animal's nearest relative was modified (Taylor 2009). Ideally this relative is the immediate sister taxon or another specimen of the same species but at a different growth stage (as with young *Gorgosaurus* and *Tyrannosaurus*). Anterior and posterior extremes of the head, neck, trunk (coracoids to anterior edge of ilium), ilium, and tail were marked on the lateral view. The corresponding structures on the dorsal view were selected and modified to match their anteroposterior dimensions in the lateral view. Width of the surrogate dorsal view was modified based on literature- or specimen-based width measurements of available structures. For example, many transverse measurements of a juvenile *Tyrannosaurus rex* skeleton (BMR P2002.4.1; courtesy of Scott Williams) were used to modify a dorsal view of an adult (Persons and Currie

PeerJ Preprints | https://doi.org/10.7287/peerj.preprints.27021v1 | CC BY 4.0 Open Access | rec: 4 Jul 2018, publ: 4 Jul 2018

2011a). The distal portion of the tail in *Yangchuanosaurus* was modeled on the more complete tail of *Sinraptor hepingensis*.

If a dorsal view of only the skull was available for a given dinosaur, and a dorsal view of the skeleton was only available for a related taxon, the differential in skull widths between the taxa was applied to the entire dorsal view of the relative's skeleton. When possible we used transverse widths of occipital condyles and frontals, measured by author PJC, to confirm ratios of total reconstructed skull widths. The width of the occipital condyle reflects width of the atlas and postaxial cervical vertebrae, and hence influences width of remaining vertebrae as well. This wholesale modification of body width is therefore tentative, but uses the best-constrained available data, and is testable with future, more complete descriptions and measurements of theropod postcrania. We applied this method for dorsal reconstructions of *Sinraptor*, *Eustreptospondylus*, *Dilophosaurus*, *Tarbosaurus*, and one juvenile *Gorgosaurus*. For example, for *Eustreptospondylus* the skull width from Walker (1964) was used to modify a dorsal reconstruction of *Allosaurus*, and the skull width of *Sinraptor hepingensis* was applied to a dorsal view of its close relative *Yangchuanosaurus shangyouensis*. Ribcage width in individual animals varies with ventilatory movements, but width variations of +/- 10% (Henderson and Snively 2003, Bates et al. 2009) have sufficiently small effect on MMI to permit statistically valid comparisons (see Henderson and Snively 2003).

We also digitized the hind legs of the specimens, by extending their skeletons and soft tissue outlines to obtain anterior and posterior coordinates. We applied a uniform semi-minor axis in the mediolateral direction, as a radius from the midline of the femur to the lateral extent of its reconstructed musculature (Paul 1988, 2010). The anterior and posterior points on the ilium constrained the maximum anteroposterior extent of the thigh muscles (Hutchinson et al. 2005),

PeerJ Preprints | https://doi.org/10.7287/peerj.preprints.27021v1 | CC BY 4.0 Open Access | rec: 4 Jul 2018, publ: 4 Jul 2018

239 which we tapered to their insertions at the knee. The anterior point of the cnemial crest
240 constrained the anterior extent of the crural muscles, but the posterior contours were admittedly
241 subjective. In Paul's (1988, 2010) reconstructions, the posterior extent of the m. gasctrocnemius
242 complex in lateral view (bulge of the "drumstick" muscles) generally correlates with the width of
243 the distal portion of the femoral shaft, where two bellies of these muscles originate. Masses of
244 both legs were added to that of the axial body to obtain total body mass. Forelimbs were not
245 included, because they could not be digitized for all specimens and add proportionally little to
246 overall mass moments of inertia (Henderson and Snively 2003, Bates et al. 2009a). The reduced
247 forelimbs of tyrannosaurids would likely add less to overall body MMI than the larger forelimbs
248 of other large theropods, especially with shorter glenoacetabular distance in tyrannosaurids (Paul
249 1988). However, even the robust forelimbs of *Acrocanthosaurus*, for example, would contribute
250 only 0.15% of the MMI of its entire axial body (Bates et al. 2009a).

251 *Mass property estimates*

252 *Volume and mass*

253 Body volume, mass, center of mass (COM), and mass moment of inertia were calculated
254 using methods similar to those of Henderson (1999), Motani (2001), Henderson and Snively
255 (2003), Durkin and Dowling (2006), and Arbour (2009). Body segments were approximated as
256 frusta (truncated cones), and volume of the axial body calculated as the sum of volumes of
257 constituent frusta (mass estimates incorporated regional densities of the body; see below).
258 Coordinates for midsagittal and coronal outlines were used to calculate radii for anterior and
259 posterior areas of each frustum. Arbour (2009) thoroughly explains the equations and procedures
260 for calculating volume of conical frusta. Equation 1 is for volume of an elliptical frustum, in
261 notation of radii (r) and length (l).

PeerJ Preprints | https://doi.org/10.7287/peerj.preprints.27021v1 | CC BY 4.0 Open Access | rec: 4 Jul 2018, publ: 4 Jul 2018

1) $$V = \frac{\pi}{3} \times l\left(r_{ant}^{DV} r_{ant}^{LM} + r_{post}^{DV} r_{post}^{LM} + \sqrt{r_{ant}^{DV} r_{ant}^{LM} r_{post}^{DV} r_{post}^{LM}}\right)$$

The superscript *DV* refers to a dorsoventral radius, and *LM* the lateral-to-midsagittal dimension (Fig. 2).

This equation can be generalized to frustum face areas of any cross section (equation 2; similar to equations presented by Motani [2001] and Arbour [2009]).

2) $$V = 1/3 \times l(Area_{anterior} + Area_{posterior} + \sqrt{Area_{anterior} Area_{posterior}})$$

Using equation 2, frustum volumes can be calculated from cross sections departing from that of an ellipse. Vertebrate bodies deviate from purely elliptical transverse sections (Motani 2001). We therefore calculated areas based on a range of superellipse exponents, from 2 (that of an ellipse) to 3 (as seen in whales and dolphins), based on the derivations and correction factors of Snively (2012) and Snively et al. (2013). Exponents for terrestrial vertebrates range from 2-2.5, with 2.5 being common (Motani 2001; Snively and Russell [2007b] used 2.3). Snively (2012) and Snively et al. (2013) derived and mathematically validated constants for other superelliptical cross-sections; for example, for k=[2, 2.3, 2.4, 2.5], C=[0.7854, 0.8227, 0.8324, 0.8408]. Volumes for different cross sections were then calculated by applying these constants, as superellipse correction factors (Snively et al. 2013), to equations 1 and 2.

Frustum volumes were multiplied by densities to obtain masses, and these were summed to obtain axial-body and leg masses. For the head we applied average density of 990 kg/m^3, based on an exacting reconstruction of bone and air spaces in *Allosaurus* by Snively at al. (2013).

PeerJ Preprints | https://doi.org/10.7287/peerj.preprints.27021v1 | CC BY 4.0 Open Access | rec: 4 Jul 2018, publ: 4 Jul 2018

We used a neck density of 930 kg/m^3 and trunk density of 740 kg/m^3 similar to that of Bates et al. (2009) for the same specimen of *Allosaurus*, which also accounted for air spaces. The post-thoracic and leg densities were set to that of muscle at 1060 kg/m^3. Density and resulting mass of these anatomical regions was probably greater (even if fat is included) because bone is denser than muscle, which would result in a more posterior COM than calculated here. Rather than introduce new sets of assumptions, we provisionally chose muscle density because its value is known, and the legs (Hutchinson et al. 2011) and tail (Mallison et al. 2015) have far greater volumes of muscle than bone. All of these density values are easily modifiable in the future, as refined anatomical data for air spaces, bone densities, and bone volumes become available, such as occurred with the restoration methods of Witmer and Ridgely (2008) and Snively et al. (2013).

We also varied tail cross-sections by applying the results of Mallison et al. (2015) for the m. caudofemoralis longus and full-tail cross sections of adult *Alligator mississippiensis* and other crocodilians. Mallison et al. (2015) found that proximal cross-sections of an adult *Alligator* tail and m. caudofemoralis longus are 1.4 times greater than those previously estimated for young *Alligator* and dinosaurs (Persons and Currie (2011a). We therefore multiplied the original width of the modeled tails of theropods (see above) by 1.4 to obtain an upper estimate of tail thickness and mass.

Inter-experimenter variation in reconstruction

We checked our mass estimation method against that of Bates et al. (2009a) by digitizing their illustrations of *Acrocanthosaurus atokensis*, including the body and the animal's dorsal fin separately. The dorsal fin was restored with half a centimeter of tissue on either side the neural spines, with a bony width of approximately 4 cm that Harris (1998) reported for the twelfth

PeerJ Preprints | https://doi.org/10.7287/peerj.preprints.27021v1 | CC BY 4.0 Open Access | rec: 4 Jul 2018, publ: 4 Jul 2018

dorsal vertebra. We assumed a rectangular cross section for the fin. The digitization and mass property estimates (see below) for *Acrocanthosaurus* were purposely carried out blind to the results of Bates et al. (2009a), to avoid bias in scaling and digitizing the outline of their illustrations.

Authors DMH and ES independently digitized reconstructions and estimated mass properties of several specimens, including the legs of many specimens and axial bodies of *Ceratosaurus*, *Allosaurus*, adult *Gorgosaurus*, and *Daspletosaurus*. The software and coding differed in these attempts, and volume reconstruction equations differed slightly (Henderson 1999, Snively 2012; current paper). ES and a graduate student individually used the current paper's methods to digitize an adult *Gorgosaurus*.

Centers of mass

To test Hypothesis 1, we calculated anteroposterior and vertical position of the centers of mass (COM) of the axial bodies (not including the legs), assuming that the animal would pivot the body around this location if both legs were planted on the ground. First, we calculated the center of mass of each frustum. Equation 3 gives the anteroposterior position of each frustum's COM (COM_{AP}); r are radii of anterior and posterior frusta, and L is its length (usually designated "h" for height of a vertical frustum).

3) $$COM_{frustum\ AP} = \frac{L \times \left(r_{ant}{}^2 + 2r_{ant}r_{post} + 3r_{post}{}^2\right)}{4 \times \left(r_{ant}{}^2 + r_{ant}r_{post} + r_{post}{}^2\right)}$$

Equation 4 below is an approximation of the dorsoventral position of a frustum's center of mass ($COM_{frustum\ DV}$), from digitized y (height) coordinates of the lateral body outlines. In this equation, h_{ant} and h_{post} are the full heights (dorsoventral dimensions) of the anterior and posterior faces of the frustum, equal to twice the radii r in equation 3. The absolute value terms (first and third in

PeerJ Preprints | https://doi.org/10.7287/peerj.preprints.27021v1 | CC BY 4.0 Open Access | rec: 4 Jul 2018, publ: 4 Jul 2018

the numerator) ensure that the result is independent of whether or not the anterior or posterior face is taller.

4) $$COM_{frustum\ DV} = \frac{2 \times h_{ant}|h_{post} - h_{ant}| + {h_{ant}}^2 + h_{post}|h_{post} - h_{ant}| + h_{ant}h_{post} + {h_{post}}^2}{3 \times h_{ant} + h_{post}}$$

Equation 4 gives an exact $COM_{frustum\ DV}$, but assumes that all frustum bases are at the same height (as though they are all resting on the same surface). To obtain the y (vertical) coordinate for the COM of each animal's body, we first approximated $COM_{frustum\ DV}$ using dorsal and ventral coordinates of the anterior and posterior face of each frustum (equation 5).

(5) $$COM_{frustum\ DV} = \frac{[(y_{ant:dorsal} + y_{ant:venral}) + (y_{post:dorsal} + y_{post:venral})]}{4}$$

We obtained the center of mass COM_{body} for the entire axial body (both anteroposterior and dorsoventral), by multiplying the mass of each frustum *i* by its position, summing these quantities for all frusta, and dividing by the entire axial body mass (equation 6). This gives the anteroposterior COM_{AP} from the tip of the animal's rostrum, and the dorsoventral COM_{DV} at the depth of COM_{AP} above the ventral-most point on the animal's trunk (typically the pubic foot).

6) $$COM_{body} = \frac{\Sigma_{i=1}^{n} COM_{frustum\ i} \times m_{frustum\ i}}{m_{body}}$$

To test Hypothesis 2, we found the position of collective COM of the body and leg, $COM_{body+leg}$, which lies lateral to COM_{body} calculated in equation 6. The lateral (z) coordinate of $COM_{body\text{-}z}$ was set to 0, and that of the leg $COM_{leg\text{-}z}$ was measured as the distance from $COM_{body:z}$ to the centroid of the most dorsal frustum of the leg. Equation 7 enables calculation of $COM_{body+leg:z}$ with this distance $COM_{leg:z}$, $COM_{body:z}$, and the masses of the swing leg and axial body.

7) $$COM_{body+leg:z} = \frac{COM_{body:z}\, m_{body} + COM_{leg:z}\, m_{leg}}{m_{body+leg}}$$

PeerJ Preprints | https://doi.org/10.7287/peerj.preprints.27021v1 | CC BY 4.0 Open Access | rec: 4 Jul 2018, publ: 4 Jul 2018

352

353 *Mass moments of inertia: Hypothesis 1 (both legs planted)*

354 Mass moment of inertia for turning laterally, designated I_y, was calculated about the axial
355 body's COM by summing individual I_y for all frusta (equation 8, first term), and the contribution
356 of each frustum to the total using the parallel axis theorem (equation 8, second term).

357 8) $$I_y = \Sigma_{i=1}^{n}(\tfrac{\pi}{4})\rho_i l_i \bar{r}_{DV} \bar{r}_{LM}^{\,3} + m_i r_i^2$$

358 For calculating I_y of an individual frustum, ρ_i is its density, and l_i is its anteroposterior length.
359 The element π/4 is a constant (C) for an ellipse, with an exponent k of 2 for its equation. We
360 modified C with superellipse correction factors for other shapes (Snively et al. 2013). The
361 dimension $\bar{r}_{DV}$ is the average of dorsoventral radii of the anterior and posterior faces of each
362 frustum, and $\bar{r}_{LM}$ are the average of mediolateral radii. The mass m_i and COM of each frustum
363 were calculated using the methods described above, and distance r_i from the whole body's COM
364 to that of each frustum was estimated by adding distances between each individual frustum's
365 COM to that of frustum i.

366 *Mass moments of inertia: Hypothesis 2 (pivoting about the stance leg)*

367 Here the body and leg are pivoting in yaw about a vertical axis passing through their
368 collective center of mass $COM_{body+leg,}$ and the center of pressure of the stance foot. Here
369 rotational inertia $I_{y\ body+leg}$ about the stance leg is the sum of the four right terms in equation 9.

370 9) $$I_{y\ body+leg} = I_{y\ body} + I_{y\ leg} + m_{body} r_{COM-to-body}^{\,2} + m_{leg} r_{COM-to-leg}^{\,2}$$

371 Term 1. $I_{y\ body}$ of the axial body about its own COM;

372 Term 2. $I_{y\ leg}$ of the swing leg about its own COM (assuming the leg is straight);

373 Term 3. The axial body's mass m_{body} multiplied by the square of the distance $r_{COM\text{-}to\text{-}body}$ from its
374 COM to the collective COM of the body + swing leg ($COM_{body+leg}$);

PeerJ Preprints | https://doi.org/10.7287/peerj.preprints.27021v1 | CC BY 4.0 Open Access | rec: 4 Jul 2018, publ: 4 Jul 2018

Term 4. The swing leg's mass m_{leg} multiplied by the square of the distance $r_{COM\text{-}to\text{-}leg}$ from its COM to the collective COM of the body + swing leg ($COM_{body+leg}$).

We calculated $I_{y\ body}$ using equation 8. To calculate $I_{y\ leg}$ (equation 10), we approximate the swing leg as extended relatively straight and rotating on its own about an axis through the centers of its constituent frusta. In equation 10, $I_{y\ leg}$ is the sum of $I_{y\ frustum}$ for all individual frusta of the leg, and $I_{y\ frustum}$ is in turn simply the sum of I_x and I_z of each frustum (Durkin 2003). These are similar to the first term in equation 8, but with anteroposterior radii r_{AP} instead of the dorsoventral radius of frusta of the axial body.

10) $$I_{y\ leg} = \Sigma_{i=1}^{n}(\tfrac{\pi}{4})\rho_i l_i(\bar{r}_{AP}\bar{r}_{LM}^{3} + \bar{r}_{LM}\bar{r}_{AP}^{3})$$

Equations 11 and 12 give distance $r_{COM\text{-}to\text{-}body}$ and $r_{COM\text{-}to\text{-}leg}$ necessary for equation 9; note the brackets designating absolute values, necessary to find a distance rather than a z coordinate.

11) $$r_{COM-to-body} = |COM_{body+leg} - COM_{body}|$$

12) $$r_{COM-to-leg} = |COM_{body+leg} - COM_{leg}|$$

A Excel spreadsheet in Supplementary Information (theropod_RI_body+one_leg.xlsx) has all variables and equations for finding RI of the body plus leg.

Estimating areas of muscle origination and cross-section

We obtained proxies for muscle force by estimating areas of muscle attachment and cross-section (Fig. 2). Muscle cross-section, and therefore force, scales at a gross level with attachment area for homologous muscles between species, for example with the neck muscles of lariform birds (Snively and Russell 2007a). Enthesis (attachment) size for individual muscles does not scale predictably with force within mammalian species of small body size (Rabey et al. 2014, Williams-Hatala et al. 2016), which necessitates a more general proxy for attachment area and force correlations between taxa, across spans of evolutionary time (Moen et al. 2016).

PeerJ Preprints | https://doi.org/10.7287/peerj.preprints.27021v1 | CC BY 4.0 Open Access | rec: 4 Jul 2018, publ: 4 Jul 2018

In such interspecific comparisons, morphometrics establish correlation between muscle size and locomotor ecomorphologies (Moen et al. 2013, 2016; Tinius et al. 2018). Leg length and ilium size are associated with both muscle size and jumping performance in frogs, across biogeography, phylogeny, and evolution (Moen et al. 2013, 2016. Between species of *Anolis* lizards, the overall size of muscle attachments on the ilium correlates with necessities of force and moments in different ecomorphotypes, including small and large ground dwellers, trunk and branch climbers, and crown giants (Tinius et al. 2018).

In theropods, the ilium is the most consistently preserved element that records leg muscle origination, and is usable for estimating overall origin area of knee extensors, hip flexors, and femoral abductors (Table 2). In large theropods, these enthesis regions have similar gross morphology, including striations indicating Sharpey's fiber-rich origins for the divisions of the m. iliotibialis, and smooth surfaces for the m. iliofemoralis.

Because ilium attachment sites are similar in all theropods, as a reasonable first approximation we infer greater forces for muscles originating from ilia with substantially greater attachment areas than smaller ones (for example, twice as long and tall). Ilia of large theropod species have a preacetabular flange with a ventral projection, which some authors reconstruct as origin for an anterior head of m. iliotibialis. We include this region in area calculations, but the flange is conceivably also or alternatively an origin for m. iliocostalis, which would stabilize the trunk.

We make similar assumptions for interspecies comparisons of the major femoral retractor, the m. caudofemoralis longus (CFL). The depth of the tail ventral to the caudal ribs correlates with the cross-section of the CFL (Persons and Currie 2011a,b; Hutchinson et al. 2011, Mallison et al. 2015). Although complete tails are rarely preserved (Hone 2012), the depth of the proximal

PeerJ Preprints | https://doi.org/10.7287/peerj.preprints.27021v1 | CC BY 4.0 Open Access | rec: 4 Jul 2018, publ: 4 Jul 2018

421 portion of the tail permits a good first estimation of maximum CFL cross-section (Persons and
422 Currie 2011a, b; Mallison et al. 2015).

423 Another femoral retractor, the m. caudofemoralis brevis (CFB), originates from the brevis
424 fossa of the postacetabular region of the ilium. We chose to omit the area of origin of the CFB
425 from this analysis, because this would require a ventral view of the ilium, which is rarely figured
426 in the literature and is difficult to photograph on mounted skeletons. A dorsal view might suffice
427 as a proxy for width of the brevis fossa, but the fossa is flanked by curved alae of bone whose
428 width is obscured in dorsal view. The fossa, and presumably the origination attachment for the
429 CFB (Carrano and Hutchinson 2002), is longer in tyrannosaurids than in other theropods because
430 the ilia are longer relative to body length (Paul 1988), but not broader (Carrano and Hutchinson
431 2002; figures in Osborn 1917, Gilmore 1920, and Madsen 1976).

432 Ilium area for muscle attachment was determined for all taxa from lateral-view
433 photographs and scientific illustrations (Table 2) scaled to the size of the original specimen (Fig.
434 2). Because some muscle scars are ambiguous, the entire lateral surface of the ilium dorsal to the
435 supra-acetabular crest was considered as providing potential area for muscle origination. Images
436 were opened in ImageJ (United States National Institutes of Health, Bethesda, Maryland, USA),
437 scaled in cm to the size of the original specimens, and the bone areas outlined. ImageJ (under
438 "Measure") was used to calculate areas within the outlines in cm^2.

439 Relative cross-sections were reconstructed for the m. caudofemoralis longus (CFL),
440 although the sample size is smaller than for lateral ilium area, and not large enough for
441 comparative regressions. *Allosaurus*, *Yangchuanosaurus*, several tyrannosaurids, and
442 *Ceratosaurus* have sufficiently well-preserved tails. Allen et al. (2009) and Persons and Currie
443 (2011a) found that a good osteological predictor of CFL cross-sectional area is vertical distance

PeerJ Preprints | https://doi.org/10.7287/peerj.preprints.27021v1 | CC BY 4.0 Open Access | rec: 4 Jul 2018, publ: 4 Jul 2018

444 from the distal tip of the caudal ribs to the ventral tip of the haemal spines. The CFL is never
445 constrained in width to the lateral extent of the caudal ribs, as often previously reconstructed
446 (Persons and Currie 2011a). As a baseline estimate (see Discussion for caveats), we assumed the
447 maximum cross-section to be that at the deepest haemal spine, and that the cross-sections were
448 semi-circular (as ES personally observed in dissections by Persons and Currie 2011a) minus
449 cross-sections of the centra. This method unrealistically simplifies the attachments, ignoring that
450 the lateral and vertical limits of CFL origin are set by the intermucular septum on the caudal ribs
451 between CFL and m. ilioichiocaudalis (Persons and Currie 2011b). Also, simply estimating
452 cross-sections as a proxy for force overlooks functionally and ontogenetically important aspects
453 of intramuscular anatomy, such positive allometry of fascicle length evident in the CFL of
454 *Alligator mississippiensis* (Allen et al. 2010). However, as with using the area of the ilium as a
455 proxy for muscle cross-section and force, using tail depth ventral to the caudal ribs is based
456 directly on fossil data. Because the articulations between the haemal arch and caudal centra
457 may not be accurate in skeletal mounts, we varied depths by +/- 10% to assess their effects on
458 CFL cross section, and on indices of turning performance. As for our tail cross-section and mass
459 estimates, we also applied the same correction factor of 1.4, that Mallison et al. (2015)
460 determined for adult *Alligator*, to our estimates of m. caudofemoralis cross-sections, to set an
461 upper bound for cross-section and force.

462 *Estimates and comparisons of relative agility*

463 We developed two indices of relative agility for theropods: $Agility_{force}$ based on
464 agility/force correlations in humans (Peterson et al. 2006, Thomas et al. 2009, Weiss et al. 2010),
465 and $Agility_{moment}$ which incorporates moments or torques. In human studies, maximal muscle
466 force relative to body mass correlates inversely with the time athletes take to complete an

PeerJ Preprints | https://doi.org/10.7287/peerj.preprints.27021v1 | CC BY 4.0 Open Access | rec: 4 Jul 2018, publ: 4 Jul 2018

obstacle course, which involves rapid changes of direction. Because force is a close direct correlate of agility in humans, independent of torque or power, we were confident in applying force to theropod agility. For $Agility_{force}$ (equation 13), we divided proxies for overall muscle force (area of muscle origin on the ilium, and cross-section estimates for the m. caudofemoralis longus) by I_y, mass moment of inertia about the y axis through the axial body's center of mass and a measure of the difficulty of turning the body. This is a comparative index of turning ability, rather than a specific biomechanical quantity.

13) $$Agility_{force} = A_{ilium} / I_y$$

Here A_{ilium} is the area (cm^2) of the ilium in lateral view. To compare this index of turning ability across theropods, we plotted the results for $Agility_{force}$ against $\log_{10}$ of body mass for tyrannosaurs and non-tyrannosaurs.

To obtain $Agility_{moment}$, we first assumed that moment arms scale as $mass^{1/3}$ (an inverse operation of Erickson and Tumanova's [2000] Developmental Mass Extrapolation). $Mass^{1/3}$ approximates isometric scaling of moment arms relative to linear size of the animals, which Bates et al. (2012) found to be the likely relationship for allosauroids. Applying this relationship to all of the theropods, we calculated an index of comparative moments, $\tau_{relative}$, using equation 14,

14) $$\tau_{relative} = (m^{1/3}/100) \times Area_{ilium} \times 20\ N/cm^2,$$

where m is body mass in kg, $Area_{ilium}$ is ilium area in cm^2, and 20 N/cm^2 is a sub-maximal concentric specific tension (Snively and Russell 2007b). In SI units, $m^{1/3}$ gives unrealistic

PeerJ Preprints | https://doi.org/10.7287/peerj.preprints.27021v1 | CC BY 4.0 Open Access | rec: 4 Jul 2018, publ: 4 Jul 2018

487 moment arms on the order of many meters for larger taxa. Dividing by 100 brings relative
488 moment arms into the more intuitive range of fractions of a meter. This is an arbitrary linear
489 adjustment that (1) does not imply that we have arrived at actual moment arms or torques during
490 life, and yet (2) maintains proportions of $\tau_{relative}$ among the taxa. $Agility_{moment}$ is $\tau_{relative}$
491 divided by *I*y (equation 15), which gives an index of angular acceleration.

492 15) $Agility_{moment} = \tau_{relative} / I_y$

493 The quantity $\tau_{relative}$ does not use actual moment arms, and is not intended for finding
494 angular accelerations. However, our index of relative moment arm lengths is anchored in the
495 isometric scaling of moment arms that Bates et al. (2012) found for allosauroids, and will be
496 testable with more exact estimates from modeling studies. A rich literature directly assesses
497 moment arm lengths in dinosaurs and other archosaurs (e.g. Hutchinson et al. 2005, Bates and
498 Schachner 2012, Bates et al. 2012, Maidment et al. 2013), and such methods will be ideal for
499 future studies that incorporate estimates of moment arms of individual muscles.

500 *Visualization of agility comparisons*

501 Although log transformation of mass is useful for statistical comparisons, plotting the raw
502 data enables intuitive visual comparisons of tyrannosaur and non-tyrannosaur agility, and
503 immediate visual identification of outliers (Packard et al. 2009). We plotted raw agility index
504 scores against $\log_{10}$ body mass in JMP (SAS Institute), which fitted exponential functions of
505 best fit to the data.

506 *Statistical comparison of group differences: phylogenetic ANCOVA*

PeerJ Preprints | https://doi.org/10.7287/peerj.preprints.27021v1 | CC BY 4.0 Open Access | rec: 4 Jul 2018, publ: 4 Jul 2018

Phylogenetic ANCOVA (phylANCOVA) enabled us to simultaneously test the influence of phylogeny and ontogeny on agility in monophyletic tyrannosaurs versus a heterogeneous group of other theropods. The phylANCOVA mathematically addresses phylogenetically distant specimens or size outliers that would require separate, semi-quantitative exploration in a non-phylogenetic ANCOVA.

Phylogenetic approach

All phylogenetically-inclusive analyses were conducted using the statistical program R (R Core Team, 2015). For our phylogenetic framework, we used a combination of consensus trees: Carrano et al. (2012) for the non-tyrannosauroid taxa (their analyses include the tyrannosauroid *Proceratosaurus*), and Brusatte and Carr (2016) for Tyrannosaurioidea, which uses *Allosaurus* as an outgroup. Multiple specimens within the same species (for *Tyrannosaurus rex* and *Tarbosaurus bataar*) were treated as hard polytomies (*sensu* Purvis and Garland, 1993; Ives *et al.*, 2007). Basic tree manipulation was performed using the {ape} package in R (version 3.5, Paradis *et al.*, 2004). Branch lengths were calculated by time-calibrating the resultant tree, as follows. First and last occurrences were downloaded from Fossilworks.org (see SI file for Fossilworks citations). Specimens within the same species were further adjusted according to their locality-specific intervals. Time calibration followed the equal-rate-sharing method of Brusatte *et al.* (2008), which avoids zero-length branches by using a two-pass algorithm to build on previously established methods (e.g. Norell, 1992; Smith, 1994; Ruta *et al.*, 2006). This arbitrarily resolved same-taxon polytomies by assigning near-zero-length branches to the base of each species. The near-zero-length branches effectively maintain the hard polytomy while facilitating transformations of the non-ultrametric variance-covariance matrix.

Determining strength of phylogenetic signal and appropriateness of phylogenetic regression

PeerJ Preprints | https://doi.org/10.7287/peerj.preprints.27021v1 | CC BY 4.0 Open Access | rec: 4 Jul 2018, publ: 4 Jul 2018

To determine whether phylogenetic regression was necessary when analyzing theropod agility, we calculated Pagel's λ (Pagel 1999) for each trait examined. Phylogenetic signal was estimated using the R package {phytools} (Revell, 2012). We found that phylogenetic signal was high for all traits ($\lambda_{\text{agility force}} = 0.89$; $\lambda_{\text{agility moment}} = 0.90$; $\lambda_{\text{mass}} = 0.88$), emphasizing the need for phylogenetically-informed regression and analysis of covariance.

Phylogenetically informed analyses

A combination of phylogenetically-informed generalized least squares (PGLS) regression and phylogenetic analysis of covariance (phylANCOVA) was used to test for significant deviations from allometric predictions for both agility force and agility moment (Garland *et al.*, 1993; Smaers and Rohlf, 2016). The PGLS model calculates the slope, intercept, confidence, and prediction intervals following a general linear model, adjusting expected covariance according to phylogenetic signal (in this case, Pagel's λ; Pagel 1999; for a recent discussion of PGLS methodology, see Symonds and Blomberg 2014). PGLS regression was conducted using the R package {caper} (Orme et al., 2013), which implements regression analysis as outlined by Freckleton and colleagues (2002). We then tested for significant departures from allometry using the recently-derived phylogenetic ANCOVA method of Smaers and Rohlf (2016). In standard ANCOVA methodologies, comparisons are made outside of a least-squares framework (Garland *et al.*, 1993; Garland and Adolph 1994; Smaers and Rohlf, 2016). As implemented in the R package {evomap} (Smaers, 2014), phylogenetic ANCOVA compares differences in residual variance in conjunction with the phylogenetic regression parameters (Smaers and Rohlf, 2016). This enables a direct least-squares test comparing the fit of multiple grades relative to a single grade (Smaers and Rohlf 2016). We assigned three groups using indicator vectors:

PeerJ Preprints | https://doi.org/10.7287/peerj.preprints.27021v1 | CC BY 4.0 Open Access | rec: 4 Jul 2018, publ: 4 Jul 2018

554 Tyrannosauridae, putative juveniles within Tyrannosauridae (hereafter "juveniles"), and non-
555 tyrannosaur theropods (hereafter "other theropods"). GLS standard errors were used to directly
556 test for significant differences in intercept and slope between groups, within a generalized
557 ANCOVA framework (Smaers and Rohlf, 2016). We tested the following groupings: 1) Among
558 groups (Tyrannosauridae vs. juveniles vs. other theropods); 2) juveniles vs. Tyrannosauridae; 3)
559 Tyrannosauridae vs. other theropods. For each of these comparisons, the phylANCOVA applied
560 F-tests to partitioned group means. This analysis was performed twice: once for $Agility_{force}$ and
561 again for $Agility_{moment}$.

562 *Standard for rejecting a null hypothesis of equal agilities*

563 Complications of phylogeny, ontogeny, and biomechanics necessitate a high statistical
564 standard for comparing agility results between sample groups. Reconstructing anatomy and
565 function in fossil animals has potential for many biases — including scaling errors, anatomical
566 judgment in reconstructions and digitizing, fossil incompleteness, and variation in muscle
567 anatomy. If one group appeared to have greater agility than the other, we tested the null
568 hypothesis (no difference) with conditional error probabilities $\alpha(p)$ (Berger and Sellke 1987,
569 Sellke et al. 2001), a Bayesian-derived standard appropriate for clinical trials in medicine.
570 Conditional error probabilities give the likelihood of false discoveries/false positive results
571 (Colquhoun 2014), effectively the likelihood that the null hypothesis is true, regardless of the
572 original distribution of the data. When p=0.05 in idealized comparisons of only two groups, the
573 probability of false discoveries approaches 29% (Colquhoun 2014). We therefore considered
574 ANCOVA group means to be definitively different if p was in the range of 0.001, at which the
575 probability of a false positive is 1.84% (Colquhoun 2014). We calculated conditional error
576 probabilities $\alpha(p)$ using equation 16 (modified from Sellke et al. [2001]), which employs the

PeerJ Preprints | https://doi.org/10.7287/peerj.preprints.27021v1 | CC BY 4.0 Open Access | rec: 4 Jul 2018, publ: 4 Jul 2018

originally calculated *p* value from the ANCOVA.

16) $\alpha(p) = \left(1 + \left[-ep\ln(p)\right]^{-1}\right)^{-1}$

Results

Mass properties and comparison with other studies

Masses, centers of mass, and mass moments of inertia are listed in Tables 3 and 4. “Best estimate” masses (Table 3) are reported for a common cross-sectional shape of terrestrial vertebrates (with a superellipse exponent of 2.3). Here we report and compare individual results, and compare between groups below, under the sections "*Regressions of agility indices versus body mass*" and "*Results of phylogenetic ANCOVA*". Inter-experimenter error was negligible. For example, leg masses converged to within 1% when reconstructions were identically scaled, and center of mass for *Daspletosaurus* was within +/- 0.4 mm.

Volumes and masses show broad agreement between our results and those calculated in other studies, such as by laser scanning of skeletal mounts (Bates et al. 2009a,b; Hutchinson et al. 2011) and fitting splines between octagonal hoops or more complex cross-sections. Our estimates of axial body mass (not including the legs) of *Acrocanthosaurus* ranged from 4416 kg (elliptical cross sections with k=2) to 4617 kg (k=2.3 super-ellipse exponent), compared with the 4485 kg best-estimate result of Bates et al. (2009a). A slender-model body+legs mass estimate of *Tyrannosaurus rex* specimen FMNH PR 2081 yielded 8302-8692 kg depending on superellipse cross section, compared with Hartman’s (2013) GDI estimate of 8400 kg. A 13% broader model (applying the breadth of the mount’s ribcage to our entire dorsal view) yielded 9131 kg, similar to Hutchinson et al.’s (2011) estimate of 9502 kg (their “lean” reconstruction: Hutchinson et al. 2011). Our largest model (Fig. 1), with an anatomically plausible 40% broader tail (Mallison eat

PeerJ Preprints | https://doi.org/10.7287/peerj.preprints.27021v1 | CC BY 4.0 Open Access | rec: 4 Jul 2018, publ: 4 Jul 2018

al. 2015) and 13% broader ribcage, yielded 9713 kg. The current study's results for the juvenile *Tyrannosaurus* BMR 2002.4.1 vary between 575 and 654 kg, from -10% to +2.3% of the 639 kg "lean model" estimate of Hutchinson et al. (2011). Volumes for *Tyrannosaurus* and *Giganotosaurus* are lower than those calculated by Henderson and Snively (2003) and Therrien and Henderson (2007), because leg width was narrower in the current study. However, the broad-model volume estimate for the large *Tyrannosaurus* converges with the narrow-ribcage model used in Henderson and Snively's (2003) sensitivity analysis, suggesting reasonable precision given inevitable errors of reconstruction.

Relative mass moments of inertia for tyrannosaurids and non-tyrannosaurids did not change with the upper-bound correction factor of 1.4 times the tail cross-sectional area (Mallison et al. 2015) and mass. However, absolute masses of the entire bodies increased by 5-7% in the tyrannosaurids and most allosauroids, and by 17% in *Acrocanthosaurus*. With this adjustment to tail cross-section, our mass estimates for the *Tyrannosaurus* specimens fell within the lower part of the range that Hutchinson et al. (2011) calculated for the largest specimen of this taxon. Centers of mass shifted posteriorly by 5-15% (greatest for *Allosaurus*), placing them closer to the anteroposterior location of the acetabulum. The centers of mass were anteroposteriorly coincident with the acetabulum in the large-tail models of *Acrocanthosaurus* and *Sinraptor*. With or without an expanded tail, the CM for *Acrocanthosaurus* was found to be consistent with results of Bates et al. (2012), but to lie posterior to the position estimated by Henderson and Snively (2003).

The largest specimens, *Giganotosaurus carolinii* and the large *Tyrannosaurus rex*, are nearly two tonnes more massive than their nearest relatives in the sample. The adult *Tyrannosaurus rex* specimens are more massive than *Giganotosaurus carolinii*, corroborating

PeerJ Preprints | https://doi.org/10.7287/peerj.preprints.27021v1 | CC BY 4.0 Open Access | rec: 4 Jul 2018, publ: 4 Jul 2018

predictions of Mazzetta et al. (2004) and calculations of Hartman (2013) for the specimens. The axial body of the reconstructed *Giganotosaurus* specimen is longer, but the large legs and wide axial body of the *T. rex* specimens contribute to a greater mass overall.

Changing the depth of the tails by +/- 10% changed the mass of the tails by the same amount, but changed the overall body masses by no more than 3% (less in the tyrannosaurids, which had more massive legs). Varying tail depth changed mass moments of inertia I_y by less than 4%, too small to have an effect on trends in relative I_y in tyrannosaurids versus non-tyrannosaurids.

Mass moments of inertia including a swing leg were between 0.55 and 5.3% greater than MMI of the axial bodies alone, and agilities correspondingly lower. MMI with the swing leg increased the least with *Acrocanthosaurus*, *Giganotosaurus*, large specimens of *Tarbosaurus* and especially *Tyrannosaurus*, and (surprisingly) *Raptorex*. *Gorgosaurus* juveniles, with proportionally long legs, showed the greatest increase in MMI and drops in agility scores when pivoting on one foot.

Muscle attachments and cross-sectional estimates

Table 3 reports ilium areas of all specimens, and Table 5 gives tail dimensions and calculated cross-sectional areas for the m. caudofemoralis longus. Tyrannosaurids have 1.2-2 times the ilium area of other large theropods of similar mass (Table 3); these ratios increase substantially when only axial body mass (total minus leg mass) is considered, because tyrannosaurids have longer and more massive legs.

M. caudofemoralis longus cross sections vary less than ilium area between the theropods (Table 5). They were slightly greater relative to body mass in most tyrannosaurids, which have deeper caudal centra compared with other theropods. For example, the CFL area of the adult

PeerJ Preprints | https://doi.org/10.7287/peerj.preprints.27021v1 | CC BY 4.0 Open Access | rec: 4 Jul 2018, publ: 4 Jul 2018

Tyrannosaurus specimens had 1.26-1.34 times the cross-sectional areas of the *Acrocanthosaurus* and *Giganotosaurus* specimens of similar respective mass. Increasing the transverse dimensions of the m. caudofemoralis longus by 1.4 times, after Mallison et al. (2015), increases cross sectional areas by the same factor of 1.4 because tail depth did not change. Increasing tail depth by 10% predictably increased CFL area by 21%, and decreasing tail depth by 10% decreased CFL area by 19%.

Regressions of agility indices versus body mass

Figs. 3-6 show regressions for the taxa included in Tables 1 and 2. Agility index values for tyrannosaurids are higher than for non-tyrannosaurids of similar body mass. Large tyrannosaurids (between 2 and 10 tonnes) have at least twice the $Agility_{force}$ or $Agility_{moment}$ values of the non-tyrannosaurids. For theropods in the 300-700 kg range, this gap increases to 2-3 times greater agility in juvenile tyrannosaurids than in allosauroid adults of similar mass. Comparing specimens of different body masses, tyrannosaurids have similar agility values to those of other theropods about half their size.

Results of phylogenetic ANCOVA

Across all variables, we estimated that much of theropod agility covariance structure can be attributed to phylogenetic affiliation (all $\lambda > 0.88$). The PGLS regression models indicate a strong relationship between agility and mass (Figs. 4, 5), as well as low variance within agility force ($R^2_{planted} = 0.9724$; $R^2_{pointe} = 0.9703$) and agility moment ($R^2_{planted} = 0.9387$; $R^2_{pointe} = 0.9384$). The λ-adjusted PGLS regression line under-predicts agility, fitting non-tyrannosaur theropods more closely than tyrannosaurids (Figs. 4, 5), indicating that theropods as a whole are more agile than predicted by phylogeny. When 95% confidence and prediction intervals (CI and

PeerJ Preprints | https://doi.org/10.7287/peerj.preprints.27021v1 | CC BY 4.0 Open Access | rec: 4 Jul 2018, publ: 4 Jul 2018

PI) are calculated according to the phylogenetic variance structure, all tyrannosaurids at or above the 95% PI for all phylogenetic regressions (Figs. 4,5).

Overall, phylANCOVAs for both agility force and agility moment reveal significant differences among all three of our designated groups: tyrannosaurids and putative juveniles versus other theropods (Tables 6 and 7; $P_{AF\ planted} = 0.0002$; $P_{AF\ pointe} = 0.0007$; $P_{AM\ planted} = 0.0026$; $P_{AM\ pointe} = 0.0007$). When the analysis was broken into specific group-wise comparisons, tyrannosaurids were found to be distinctive from other theropods, whether in the context of agility force or agility moment (Tables 6 and 7; $P_{AF\ planted} = 0.0001$; $P_{AF\ pointe} = 0.0003$; $P_{AM\ planted} = 0.001$; $P_{AM\ pointe} = 0.0003$). Putative tyrannosaurid juveniles were not found to be significantly different than their adult counterparts for either performance metric (Tables 6 and 7; $P_{AF\ planted} = 0.4261$; $P_{AF\ pointe} = 0.5933$; $P_{AM\ planted} = 0.6409$; $P_{AM\ pointe} = 0.6031$). For this reason, juveniles are not considered apart from adults and have a similar relationship between mass and agility. Conditional error probabilities $\alpha(p)$ are between 0.002-0.018 comparisons among groups and between tyrannosaurids and other theropods, indicating a negligible probability of false positive results.

Discussion

Phylogenetic ANCOVA demonstrates definitively greater agility in tyrannosaurids relative to other large theropods examined.

Regressions of agility indices against body mass (Figs. 3-5), and especially phylogenetic ANCOVA (Figs. 4, 5), corroborate the hypotheses that tyrannosaurids could maneuver more quickly than allosauroids and some other theropods of the same mass.

PeerJ Preprints | https://doi.org/10.7287/peerj.preprints.27021v1 | CC BY 4.0 Open Access | rec: 4 Jul 2018, publ: 4 Jul 2018

689 To evaluate potential biologically-relevant distinctiveness between tyrannosaurids and
690 other theropods, we used a recently developed method of phylogenetic ANCOVA that enabled
691 group-wise comparisons in the context of the total-group covariance structure (Smaers and Rohlf,
692 2016). By preserving the covariance structure of the entire dataset, this method yields a more
693 appropriate hypothesis test for comparing groups of closely related species (as compared to
694 standard ANCOVA procedures which segregate portions the dataset and therefore compare
695 fundamentally different covariance structures; Garland *et al.*, 1993; Garland and Adolph, 1994).
696 Our phylogenetic regression analysis finds that agility and mass are strongly correlated among
697 all theropods ($R^2 > 0.94$; $P < 0.001$), and exhibit a high degree of phylogenetic signal ($\lambda > 0.88$).
698 Using the phylANCOVA of Smaers and Rohlf (2016), we were able to determine that
699 tyrannosaurids exhibit significantly higher agility metrics than other theropods (Figs. 3-5; Tables
700 6 and 7. Putative tyrannosaurid juveniles were not found to be significantly different from adults
701 and were on or within the 95% prediction interval, aligning these individuals closer to expected
702 phylogenetic structure of their adult counterparts (Figs. 4, 5; Tables 6 and 7). The slope of the
703 phylogenetic regression lines are greater than -1 but less than 0, suggesting that agility decreases
704 out of proportion to mass as theropods grow.
705 These results allow us to draw important evolutionary conclusions, highlighting the
706 possibility of locomotor niche stratification within Theropoda. The strength of phylogenetic
707 signal combined with the clear degree of separation between tyrannosaurids and non-tyrannosaur
708 theropods underscore the importance of using a phylogenetically-informed ANCOVA to
709 understand between- and within-group agility evolution. By using a phylogenetically-informed
710 analysis, we are able to confirm significant differences in turning behavior, with tyrannosaurs

PeerJ Preprints | https://doi.org/10.7287/peerj.preprints.27021v1 | CC BY 4.0 Open Access | rec: 4 Jul 2018, publ: 4 Jul 2018

possessing uniquely superior agility scores. These results could indicate a functional specialization for distinctive ecological niches among these groups.

Studies of performance evolution can be difficult because morphology doesn't always translate into performance differences (Garland and Losos, 1994; Lauder, 1996; Lauder and Reilly, 1996; Irschick and Garland, 2001; Toro *et al.*, 2004). This study, through quantification of multi-body, multifaceted performance metrics, finds strong relationships between morphology, agility, and a distinctive performance capacity by tyrannosaurids. With respect to other theropods, tyrannosaurids are increasingly agile without compromising their large body mass, such that in a pairwise comparison, tyrannosaurids are achieving the same agility performance of much smaller theropods (Figs. 3-5). For example, a 500 kg *Gorgosaurus* has slightly greater agility scores than the 200 kg *Eustreptospondylus*, and an adult *Tarbosaurus* nearly twice the agility scores of the lighter *Sinraptor* This agility performance stratification suggests that these two groups may have had different ecologies, inclusive of both feeding and locomotory strategies. Further, by including juveniles in our analysis through the use of independent inclusion vectors, we were further able to estimate performance capacity in younger life history stages. This revealed that agility performance is established relatively early in life and carries through to large adult body masses.

This quantitative evidence of greater agility in tyrannosaurids is robust, but requires the consideration of several caveats. Agility scores rest on the relationships between agility and muscle force, and muscle force and attachment area. Muscle force and agility correlate directly with each other in humans (Peterson et al. 2006, Thomas et al. 2009, Weiss et al. 2010), and at a gross level muscle cross-sectional area and force scale with the size of muscle attachments (Snively and Russell 2007a). However, these correlations have yet to be studied in the same

PeerJ Preprints | https://doi.org/10.7287/peerj.preprints.27021v1 | CC BY 4.0 Open Access | rec: 4 Jul 2018, publ: 4 Jul 2018

system; for example linking ilium area to force and agility in humans. More thorough testing of the hypothesis will require detailed characterization of muscle sizes, forces and moments in theropods (Hutchinson et al. 2007, 2011). However, based on dramatic and statistically robust differences between tyrannosaurids and other theropods (Figs. 3-6), we predict that refined studies will corroborate discrepancies in relative agility. Furthermore, we predict that with the same methods, the short-skulled, deep-tailed abelisaurids will have agility indices closer to those of tyrannosaurids than to the representatives of the predominantly allosauroid sample we examined.

Theropod mass property estimates are consistent between diverse methods, suggesting reliable inferences about relative agility.

Theropod mass and MMI estimates in this study converge with those of other workers, despite differing reconstructions and methods. Our mass estimates for one large *Tyrannosaurus rex* (FMNH PR 2081) are within + or - 6% of the "lean" estimate of Hutchinson et al. (2011), who laser scanned the mounted skeleton with millimeter-scale accuracy. Hutchinson et al.'s (2011) models of this specimen probably have more accurate dorsoventral tail dimensions than ours, with a relatively greater depth corresponding to that of extant sauroposids (Allen et al. 2009), whereas our models have broader tails. Our mass estimate for the "Jane" specimen (BMR 2002.4.1) was similarly close. These convergences are remarkable, considering that we conducted our estimates long before we were aware of this parallel research, and using a different method. Depending on assumed cross-sections, our axial body estimates for *Acrocanthosaurus* ranged from -1.6% to +2.9% of those of Bates et al. (2009b), which were obtained from laser scanning for linear dimensions, and lofted computer models for volume. As for our estimates of *Tyrannosaurus* mass properties, the *Acrocanthosaurus* calculations were

PeerJ Preprints | https://doi.org/10.7287/peerj.preprints.27021v1 | CC BY 4.0 Open Access | rec: 4 Jul 2018, publ: 4 Jul 2018

757 "blind" to Bates et al.'s (2009a) results for this specimen. For all of the examined taxa, volumes
758 of the neck and width of the base of the tail are likely greater in our study than in others, even
759 with robust models in their sensitivity analyses (Hutchinson et al. 2007; Bates et al. 2009a,b),
760 because our models incorporate new anatomical data on soft tissues (Snively and Russell 2007b,
761 Allen et al. 2009, Persons and Currie 2010, Mallison et al. 2015) indicating a taller, broader neck
762 and broader tail cross-sections. Despite these discrepancies in soft tissue reconstruction, high
763 consistency with methods based on scanning full-sized specimens engenders optimism about the
764 validity of frustum-method estimates (Henderson 1999), despite their dependence on 2D images,
765 restoration accuracy, and researcher judgments about amounts of soft tissue.

766 Frustum and graphical double integration (GDI) methods also yielded similar results
767 (Appendix 1). When superellipse correction factors were applied to the 9.2 m^3 GDI volume
768 Hartman (2013) obtained for the *Tyrannosaurus rex* (PR 2081), results closer to our broad-
769 bodied volume estimate for the specimen were generated. Assuming a super-ellipse exponent of
770 2.3, scaling Hartman's (2013) estimate by the correction factor of 1.047 gives an estimate of
771 9.632 m^3, less than 2% greater than our estimate. Furthermore, applying super-ellipsoid cross
772 sections may reconcile careful GDI estimates, such as Taylor's (2009) for the sauropods
773 *Brachiosaurus* and *Giraffatitan*, with volumes evident from laser scans and photogrammetry of
774 fossil mounts (Gunga et al. 2008, Bates et al. 2016).

775 In addition to convergence of mass and volume estimates, different algorithms for center
776 of mass give nearly identical COM estimates for *Giganotosaurus*, the longest theropod in the
777 sample (see Appendix 1). The discrepancy of only 0.2 mm is negligible for a 13 m-long animal.
778 Although we recommend finding the anteroposterior COM of each frustum using our equation 4
779 (especially for rotational inertia calculations), the simpler approximation method is adequate.

PeerJ Preprints | https://doi.org/10.7287/peerj.preprints.27021v1 | CC BY 4.0 Open Access | rec: 4 Jul 2018, publ: 4 Jul 2018

780 Calculation methods probably have a smaller effect on center of mass estimates than
781 anatomical assumptions concerning restoration, and variations in the animal's postures in real
782 time. Such postural changes would include turning or retracting the head, and movements of the
783 tail (Carrier et al. 2001) using axial (Persons and Currie 2011a, b; Persons and Currie 2013) and
784 caudofemoral muscles (Bates et al. 2009; Allen et al. 2010; Persons and Currie 2011a, b;
785 Hutchinson et al. 2011; Persons and Currie 2013). The congruence of results from different
786 methods is encouraging, because biological factors govern the outcome more than the choice of
787 reconstruction method.
788 *Relative agilities are insensitive to modeling bias.*
789 Reconstruction differences between this and other studies are unlikely to bias the overall
790 comparative results so long as anatomical judgments and methods are consistently applied to all
791 taxa. For example, although tail width is reconstructed similarly in this study and the dissection-
792 based studies of Allen et al. (2010) and Persons and Currie (2011), the tail depths of our models
793 may be too shallow (Allen et al. 2010). Consistently deeper tails, better matching reconstructions
794 of Allen et al. (2010), Bates et al. (2009a, b) and Hutchinson et al. (2011), would, however, not
795 alter our overall comparative results.
796 Considering *I*y and mass from independent studies is instructive in relation to potential
797 modeling bias and error. Bates et al. (2009b) calculated notably high mass and *I*y (Hutchinson et
798 al. 2011) for a *Tyrannosaurus rex* specimen (MOR 555) not included in our study, yet with its
799 enormous ilium its agility indices would be higher than those of a non-tyrannosaurid
800 *Acrocanthosaurus* of equivalent mass (Bates et al. 2009b). *I*y and agility for the *Allosaurus*
801 examined by Bates et al. (2009a) are similar to those for other *Allosaurus* specimens. Consistent
802 modeling bias for all theropods (making them all thinner or more robust) would have no effect

PeerJ Preprints | https://doi.org/10.7287/peerj.preprints.27021v1 | CC BY 4.0 Open Access | rec: 4 Jul 2018, publ: 4 Jul 2018

on relative agility assessments. Overlap of agility would require inconsistent bias in this study and those of other workers, with more robust tyrannosaurid reconstructions and slender non-tyrannosaurids. This bias is unlikely, because reconstructions were checked against skeletal measurements and modified when necessary, and most reconstructions were drawn from one source (Paul 2010).

Furthermore, the current mass estimates cross-validate those of Campione et al.'s (2014) methods based on limb circumference-to-mass scaling in bipeds. Our lower mass estimate (6976 kg) for one adult *Tyrannosaurus rex* specimen (AMNH 5027) coincides remarkably with their results (6688 kg), considering the large tail width of our reconstruction. These close correspondences of inertial properties between different studies gives confidence for biological interpretation.

Behavioral and ecological implications of agility in large theropods

This discrepancy in agility between tyrannosaurids and other large theropods raises specific implications for prey preference, hunting style, and ecology. By being able to maneuver faster, tyrannosaurids were presumably more adept than earlier large theropods in hunting relatively smaller (Hone and Rauhut 2009), more agile prey, and/or prey more capable of active defense. This capability in tyrannosaurids is consistent with coprolite evidence that indicates tyrannosaurids fed upon juvenile ornithischians (Chin et al. 1998, Varricchio 2001), and with healed tyrannosaurid bite marks on adult ceratopsians and hadrosaurs (Carpenter 2000, Wegweiser et al. 2004, Happ 2008). Tyrannosaurids co-existed with herbivorous dinosaurs that were predominately equal to or smaller than them in adult body mass. The largest non-tyrannosaurids, including *Giganotosaurus*, often lived in habitats alongside long-necked sauropod dinosaurs, the largest land animals ever. These associations suggest that allosauroids

PeerJ Preprints | https://doi.org/10.7287/peerj.preprints.27021v1 | CC BY 4.0 Open Access | rec: 4 Jul 2018, publ: 4 Jul 2018

826 may have preferred less agile prey than did tyrannosaurids. It is also possible that stability
827 conferred by high rotational inertia, as when holding onto giant prey, was more important for
828 allosauroids than turning quickly.

829 These faunal correspondences between predator agility and adult prey size are not
830 absolute, however. Tyrannosaurids sometimes shared habitats with large sauropods (Nemegt,
831 Ojo Alamo, and Javalina Formations: Borsuk-Białynicka 1977, Lehman and Coulson 2002,
832 Sullivan and Lucas 2006, Fowler and Sullivan 2011), and even with exceptionally large
833 hadrosaurids (Hone et al. 2014). Relative agility of herbivorous dinosaurs must be tested
834 biomechanically to assess the possible advantages of agility in tyrannosaurids. Snively et al.
835 (2015) calculated that ceratopsians had lower MMI, and hadrosaurs and sauropods greater MMI,
836 than contemporaneous theropods, but musculoskeletal turning ability has yet to be assessed in
837 detail for dinosaurian herbivores.

838 Tyrannosaurids were unusual in being the only toothed theropods (thus excluding large-
839 to-giant oviraptorosaurs and ornithomimosaurs) larger than extant wolves in most of their
840 habitats (Farlow and Holtz 2002, Farlow and Pianka 2002, Holtz 2004). Among toothed
841 theropods, adult tyrannosaurids of the Dinosaur Park Formation were 50-130 times more
842 massive than the next largest taxa (troodontids and dromaeosaurids: Farlow and Pianka 2002).
843 Comparing the dromaeosaur *Dakotaraptor steini* (DePalma et al. 2015) and *Tyrannosaurus rex*
844 in the Hell Creek formation reveals an instructive minimum discrepancy. We estimate the mass
845 of *Dakotaraptor* to be 374 kg, using the femoral dimensions provided by DePalma et al. (2015:
846 Fig. 9) and the equations of Campione et al. (2014). Adult *Tyrannosaurus* attained 17-24 times
847 this mass (our estimates), approximately the difference between a large male lion and an adult

PeerJ Preprints | https://doi.org/10.7287/peerj.preprints.27021v1 | CC BY 4.0 Open Access | rec: 4 Jul 2018, publ: 4 Jul 2018

848 black backed jackal. By our estimates, the juvenile *Tyrannosaurus* in our sample was nearly
849 twice as massive as an adult *Dakotarapor*.

850 These size differences between adult tyrannosaurids and non-tyrannosaurid predators
851 suggest that subadult tyrannosaurids were able to capably hunt midsized prey, in ecological roles
852 vacated by less-agile, earlier adult theropods of similar body mass. In contrast, many earlier
853 faunas (Foster et al. 2001, Farlow and Holtz 2002, Farlow and Pianka 2002, Russell and Paesler
854 2003, Holtz 2004, Foster 2007, Läng et al. 2013; although see McGowen and Dyke 2009) had a
855 continuum of body masses between the largest and smallest adult theropods, and perhaps greater
856 subdivision of niches between adults (Läng et al. 2013). A companion paper (Surring et al., in
857 revision) explores alternative evolutionary scenarios, and presents soft-tissue evidence in a
858 further exploration of tyrannosaurid agility.

859 **Appendix**

860 *How precise are different methods of mass property estimation?*

861 In addition to our mathematical slicing procedures (Henderson 1999), methods for
862 calculating mass properties include use of simplified B-splines or convex hulls to represent body
863 regions (Hutchinson et al. 2007, Sellers et al. 2012, Brassey and Sellars 2014, Brassey et al.
864 2016), or more complex NURBS (non-uniform rational B-spline) reconstruction modified to fit
865 the contours of mounted skeletons and inferred soft tissues (Bates et al. 2009a, b; Mallison 2007,
866 2010, 2014; Stoinsky et al. 2011). Brassey (2017) reviews and compares these methods in detail.
867 Both spline-based and mathematical slicing methods have been validated for living terrestrial
868 vertebrates (Henderson 1999, 2004, 2006; Henderson and Snively 2003, Hutchinson et al. 2007,
869 Bates et al. 2009a). However, spline-based methods [as in Mallison's (2007, 2010, 2014) and
870 similar procedures] are conceivably more accurate than slicing methods, which are based on a

PeerJ Preprints | https://doi.org/10.7287/peerj.preprints.27021v1 | CC BY 4.0 Open Access | rec: 4 Jul 2018, publ: 4 Jul 2018

few extreme coordinates of the body, and estimate intermediate contours as ellipses or non-ellipsoid superellipses (Henderson 1999, Motani 2001, Henderson and Snively 2003, Arbour 2009, Snively et al. 2013). We compared results of mathematical slicing and spline methods by obtaining inertial properties from both slicing abstractions and spline models of several theropods, based on the dimensions used in the slicing calculations.

Another method, termed graphical double integration (GDI; Jerison 1973), uses elliptical cylinders instead of frusta to estimate volumes. For reptiles with cylindrical bodies, GDI approximates mass better than regressions based on body length or bone dimensions (Hurlburt 1999). Masses and *I*y were calculated by GDI for all specimens, and compared to results from the frustum method.

Methods for testing precision of mass property results from different approaches

To compare slicing and spline-based inertial property results of full axial bodies of theropods, we constructed spline models of *Yangchuanosaurus shangyouensis*, *Sinraptor hepingensis*, and *Tarbosaurus bataar* (Fig. 6), after Snively et al. (2013) and Snively et al. (2015). We used FreeCAD (freecadweb.org) to construct the bodies from lofted ellipses, and MeshLab (meshlab.sourceforge.net) to obtain volume, centers of mass, and the inertia tensor, assuming uniform densities.

We further estimated volumes of *Eustreptospondylus oxoniensis* and *Yanchuanosaurus shangyouensis* using the graphical double integration methods of Jerison (1973), Hurlburt (1999), Murray and Vickers Rich (2004), and Taylor (2009), using equation 12.

12) $$V_{body} = \Sigma_{n=1}^{i} V_i = \pi(r_{i1})(r_{i2})L_i$$

The body is divided into segments from 1 to i. Each body segment is treated as an elliptical cylinder with the cross sectional area of its anterior ellipse, with major and minor radii of r_1 and

PeerJ Preprints | https://doi.org/10.7287/peerj.preprints.27021v1 | CC BY 4.0 Open Access | rec: 4 Jul 2018, publ: 4 Jul 2018

894 r_2. This area is multiplied by L, the segment's length as the distance to the subsequent ellipse.

895 We also tested convergence of body COM approximations using COM of each frustum
896 (equation 4), versus simply assuming that each frustum's anterioposterior COM was very close
897 to its larger-diameter face. The longest specimen, *Giganotosaurus carolinii*, was the best
898 candidate for this test because I_y is sensitive to the square of the distance r (equation 8) of a
899 segment's COM from the body total COM. The distance of the large-diameter face from the
900 animal's rostrum was used as the value for $COM_{frustum}$ in equation 7.

901 *Results of methods comparison*

902 Values of mass and mass moment of inertia varied little between methods using frusta
903 (truncated cones), extruded ellipses (GDI), and spline (3D lofting) methods. Volumes, COM, and
904 MMI (assuming uniform density) were within 0.5% of each other for frustum and spline models
905 of *Sinraptor hepingensis*, *Yangchuanosaurus shangyouensis*, and *Tarbosaurus bataar* (Fig. 6).
906 The GDI mass and MMI for *Eustreptospondylus oxoniensis* were only 0.1% higher than
907 calculated by the frustum method, and that for *Yanchuanosaurus shangyouensis* only 0.5%
908 higher. However, differences increase substantially for estimates of hind limb mass. GDI-
909 calculated mass for the hind leg of *Eustreptospondylus* is over 11% greater than that from the
910 frustum method.

911 GDI and frustum estimates are closest for axial bodies of the theropods, but diverged for
912 the hind legs. This suggests high accuracy of the method for relatively tubular objects, such as
913 the bodies of some sprawling tetrapods (Hurlburt 1999), and the necks, tails, and legs of giant
914 long-necked sauropod dinosaurs (Taylor 2009). GDI with extruded ellipses is less accurate for
915 highly tapered objects, such as the hind legs of theropods, the trunks of some large theropods and
916 sauropods, and other animals with ribcages that flare laterally in coronal section. However, the

PeerJ Preprints | https://doi.org/10.7287/peerj.preprints.27021v1 | CC BY 4.0 Open Access | rec: 4 Jul 2018, publ: 4 Jul 2018

high frequency of body cross sections (Motani 2001), as in our axial body models, ameliorates the potential error of GDI for tapered objects.

For the *Giganotosaurus* model, the position of COM_{body} from the tip of the rostrum was identical to three significant figures, whether using equation 4 or assuming that each frustum's COM was very close to its larger face (4.65665 m versus 4.65685 m, a difference of 2 $x10^{-4}$ m).

References

Allen V., Paxton H., and Hutchinson J.R. 2009. Variation in center of mass estimates for extant sauropsids and its importance for reconstructing inertial properties of extinct archosaurs. *Anatomical Record* 292: 1442-1461.

Arbour V.M. 2009. Estimating impact forces of tail club strikes by ankylosaurid dinosaurs. *PLoS ONE* 4(8): e6738. doi:10.1371/journal.pone.0006738

Bakker R.T. and Bir G. 2004. Dinosaur crime scene investigations: theropod behavior at Como Bluff, Wyoming, and the evolution of birdness. In: Currie P.J., Koppelhus E.B., Shugar M.A., and Wright J.L. (eds). *Feathered dragons: Studies on the Transition from Dinosaurs to Birds*. pp. 301-342. Indiana University Press, Bloomington.

Bates K.T., Falkingham P.L., Breithaupt B.H., Hodgetts D., Sellers W.I. and Manning P.L. 2009a. How big was 'Big Al'? Quantifying the effect of soft tissue and osteological unknowns on mass predictions for *Allosaurus* (Dinosauria:Theropoda). *Palaeontologia Electronica Vol.* 12, Issue 3; 14A: 33p; http://palaeo-electronica.org/2009_3/186/index.html

Bates K.T., Manning P.L., Hodgetts D., and Sellers W.I. 2009b. Estimating mass properties of dinosaurs using laser imaging and 3D computer modelling. PLoS ONE 4(2): e4532. doi:10.1371/journal.pone.0004532

Bates K.T., Mannion P.D., Falkingham P.L., Brusatte S.L., Hutchinson J.R., Otero A., Sellers W.I., Sullivan C., Stevens K.A., and Allen V. 2016. Temporal and phylogenetic evolution of the sauropod dinosaur body plan. *Royal Society Open Science* 3: 150636.

PeerJ Preprints | https://doi.org/10.7287/peerj.preprints.27021v1 | CC BY 4.0 Open Access | rec: 4 Jul 2018, publ: 4 Jul 2018

954 Bates K.T. and Schachner E.R. (2012). Disparity and convergence in bipedal archosaur
955 locomotion. *Journal of the Royal Society Interface* 9: 1339–1353.
956
957 Bates K.T., Benson R.B.J., and Falkingham P.L. 2012. A computational analysis of locomotor
958 anatomy and body mass evolution in Allosauroidea (Dinosauria: Theropoda). *Paleobiology* 38:
959 486-507.

960 Berger J.O. and Sellke T. 1987 Testing a point null hypothesis: the irreconcilability of p-values
961 and evidence. *Journal of the American Statistical Association* 82: 112–122.

962 Borsuk-Białynicka M.M. 1977. A new camarasaurid sauropod *Opisthocoelicaudia skarzynskii*
963 gen. n., sp. n. from the Upper Cretaceous of Mongolia. *Acta Palaeontologia Polonica* 37:5–64

964 Brassey C.A. 2017. Body-mass estimation in paleontology: a review of volumetric techniques.
965 *The Paleontological Society Special Papers* 22:133-156.

966 Brassey C.A., Sellers W.I. 2014. Scaling of convex hull volume to body mass in modern
967 primates, non-primate mammals and birds. PLoS ONE 9(3): e91691.

968 Brassey C.A., O'Mahoney T.G., Kitchener A.C., Manning P.L., Sellers W.I. 2016. Convex-hull
969 mass estimates of the dodo (*Raphus cucullatus)*: application of a CT-based mass estimation
970 technique. *PeerJ* 4: e1432

971 Brochu C.A. 2002. Osteology of *Tyrannosaurus rex*: insights from a nearly complete skeleton
972 and high-resolution computed tomographic analysis of the skull. *Society of Vertebrate*
973 *Paleontology Memoir* 7. *Journal of Vertebrate Paleontology* 22 (Supplement to 4): 1–138.

974 Brusatte S.L. and Carr T.D. 2016. The phylogeny and evolutionary history of tyrannosauroid
975 dinosaurs. *Scientific Reports* 6: 20252.
976
977 Brusatte S.L., Norell M.A., Carr T.D., Erickson G.M., Hutchinson J.R., Balanoff A.M., Bever
978 G.S., Choiniere J.N., Makovicky P.J., and Xu X. 2010. Tyrannosaur paleobiology: new research
979 on ancient exemplar organisms. *Science*.329: 1481-1485.
980
981 Calvo, J.O. and Coria, R.A. 1998. New specimen of *Giganotosaurus carolinii* (Coria and
982 Salgado, 1995), supports it as the largest theropod ever found. In: Pérez-Moreno B.P., Holtz
983 T.R.,Jr., Sanz J.L. and Moratalla J.J. (eds.). Aspects of Theropod Palaeobiology, Gaia Special
984 Volume. pp. 117-122.
985
986 Campione N.E., Evans D.C., Brown C.M, and Carrano M.T. 2014. Body mass estimation in non-
987 avian bipeds using a theoretical conversion to quadruped stylopodial proportions. *Methods in*
988 *Ecology and Evolution* 5: 913-923.
989
990 Carrano M.T. and Hutchinson J.R. 2002. Pelvic and hindlimb musculature of *Tyrannosaurus rex*
991 (Dinosauria: Theropoda). *Journal of Morphology* 253: 207-228.
992

PeerJ Preprints | https://doi.org/10.7287/peerj.preprints.27021v1 | CC BY 4.0 Open Access | rec: 4 Jul 2018, publ: 4 Jul 2018

PeerJ Preprints NOT PEER-REVIEWED

993 Carrano M.T., Benson R.B.J., and Sampson S.D. 2012. The phylogeny of Tetanurae (Dinosauria:
994 Theropoda). *Journal of Systematic Palaeontology* 10: 211-300.
995
996
997 Carrier D.R., Walter R.M. and Lee D.V. 2001. Influence of rotational inertia on turning
998 performance of theropod dinosaurs: clues from humans with increased rotational inertia. *Journal*
999 *of Experimental Biology* 204: 3917–3926.
1000
1001 Chin K., Tokaryk T.T., Erickson G.M., and Calk L.C. 1998 A king-sized theropod coprolite.
1002 *Nature* 393: 680–682.
1003
1004 Colquhoun D. 2014 An investigation of the false discovery rate and the misinterpretation of *p*-
1005 values. *Royal Society Open Science* 1: 140216.
1006
1007 Coria R.A. and Currie P.J. 2003. The braincase of *Giganotosaurus carolinii* (Dinosauria:
1008 Theropoda) from the Upper Cretaceous of Argentina. *Journal of Vertebrate Paleontology* 22:
1009 802-811.
1010
1011 DePalma R.A., Burnham D.A., Martin L.D., Larson P.L., and Bakker R.T. 2015. The first giant
1012 raptor (Theropoda: Dromaeosauridae) from the Hell Creek Formation. *Paleontological*
1013 *Contributions* 14: 1-16.
1014
1015 Dong Z., Zhou S., and Zhang Y. 1983. Dinosaurs from the Jurassic of Sichuan. *Palaeontologica*
1016 *Sinica* New Series C 162: 1-136.
1017
1018 Durkin J. 2003. Development of a geometric modeling approach for human body segment
1019 inertial parameters. Doctoral Thesis. McMaster University.
1020
1021 Erickson G.M. and Tumanova T.A. 2000. Growth curve of *Psittacosaurus mongoliensis* Osborn
1022 (Ceratopsia: Psittacosauridae) inferred from long bone histology. *Zoological Journal of the*
1023 *Linnean Society* 130: 551–566.
1024
1025 Farlow J.O. and Holtz T.R. Jr. 2002. The fossil record of predation in dinosaurs. In: Kowalewski,
1026 M. and P.H. Kelley (eds.). *The Fossil Record of Predation*. pp. 251-266 (The Paleontological
1027 Society Papers 8, 2002).
1028
1029 Farlow J.O. and Pianka E.R. 2002. Body size overlap, habitat partitioning and living space
1030 requirements of terrestrial vertebrate predators: implications for the paleoecology of large
1031 theropod dinosaurs. *Historical Biology* 16: 21-40.
1032
1033 Foster J. 2007. *Jurassic West*. Indiana University Press, Bloomington.
1034
1035 Foster J.R. and Chure D.J. 2006. Hindlimb geometry in the Late Jurassic theropod dinosaur
1036 *Allosaurus*, with comments on its abundance and distribution. In: Foster J.R. and Lucas S.G.
1037 (eds.), *Paleontology and Geology of the Upper Jurassic Morrison Formation*. *New Mexico*
1038 *Museum of Natural History and Science Bulletin* 36: pp. 119-122.

PeerJ Preprints | https://doi.org/10.7287/peerj.preprints.27021v1 | CC BY 4.0 Open Access | rec: 4 Jul 2018, publ: 4 Jul 2018

PeerJ Preprints NOT PEER-REVIEWED

Foster J.R., Holtz T.R. Jr., and Chure D.J. 2001. Contrasting patterns of diversity and community structure in the theropod faunas of the Late Jurassic and Late Cretaceous of Western North America. *Journal of Vertebrate Paleontology* 21(Supplement to 3): 51A.

Fowler D.W. and Sullivan R.M. 2011. The first giant titanosaurian sauropod from the Upper Cretaceous of North America. *Acta Palaeontologica Polonica* 56: 685-690.

Freckleton R.P. 2002. On the misuse of residuals in ecology: Regression of residuals vs. multiple regression. *Journal of Animal Ecology* 71: 542-545.

Gao Y. 1992. *Yanchuanosaurus hepingensis*–a new species of carnosaur from Zigong, China. *Vertebrata Palasiatica* 32: 313-324.

Garland T. and Adolph S.C. 1994. Why not to do 2-species comparative studies—limitations on inferring adaptation. *Physiologial Zoology* 67: 797–828.

Garland T. Jr. and Losos J.B. 1994. Ecological morphology of locomotor performance in squamate reptiles. In: Wainwright P.C. and Reilly S. (eds.), *Ecological Morphology: Integrative Organismal Biology*. University of Chicago Press Chicago. pp. 240-302

Garland T., Dickerman A.W., Janis C.M., and Jones J.A. 1993. Phylogenetic analysis of covariance by computer simulation. *Systematic Biology* 42: 265-292.

Gilmore, C. W. 1920. Osteology of the carnivorous Dinosauria in the United States National Museum, with special reference to the genera *Antrodemus* (*Allosaurus*) and *Ceratosaurus*. *Bulletin of the United States National Museum* 110: 1-154.

Gunga H.-C., Suthau T., Bellmann A., Stoinski S., Friedrich A., Kirsch K. and Hellwich O., 2008. A new body mass estimation of *Brachiosaurus brancai* Janensch, 1914 mounted and exhibited at the Museum of Natural History (Berlin, Germany). *Fossil Record* 11: 33-38.

Harris J.D. 1998. A reanalysis of *Acrocanthosaurus atokensis*, its phylogenetic status, and paleobiogrographic implications, based on a new specimen from Texas. *New Mexico Museum of Natural History and Science Bulletin* 13: pp. 1-75.

Hartman S. 2011. Skeletal Drawing. http://skeletaldrawing.com. Accessed August 19, 2011.

Henderson D.M. 1999. Estimating the masses and centers of mass of extinct animals by 3-D mathematical slicing. *Paleobiology* 25: 88-106.

Henderson D.M. and Snively E. 2003. *Tyrannosaurus en pointe*: Allometry minimized rotational inertia of large carnivorous dinosaurs. *Proceedings of the Royal Society B, Biology Letters* 271: S57-S60.

PeerJ Preprints | https://doi.org/10.7287/peerj.preprints.27021v1 | CC BY 4.0 Open Access | rec: 4 Jul 2018, publ: 4 Jul 2018

1085 Holtz T. R., Jr. 2004. Taxonomic diversity, morphological disparity, and guild structure in
1086 theropod carnivore communities: implications for paleoecology and life history strategies in
1087 tyrant dinosaurs. *Journal of Vertebrate Paleontology* 24(supplement to 3), 72A-72A.
1088
1089 Holtz T.R. Jr. 2002. Theropod predation: evidence and ecomorphology. In *Predator−Prey*
1090 *Interactions in the Fossil Record* (eds Kelly, P.H., Koweleski, M., and Hansen T.A) *Topics in*
1091 *Geobiology* 17. 325-340 (Kluwer/Plenum, 2002).
1092
1093 Holtz T.R., Jr. 1995. The arctometatarsalian pes, an unusual structure of the metatarsus of
1094 Cretaceous Theropoda (Dinosauria: Saurischia). *J. Vertebr. Paleontol.* 14: 480-519.
1095
1096 Hone D.W.E., Wang K., Sullivan C., Zhao X., Chen S., Li D., Ji S., Ji Q., and Xu X. 2011. A
1097 new, large tyrannosaurine theropod from the Upper Cretaceous of China. *Cretaceous Research*
1098 32: 495-503.
1099
1100 Hone D.W.E., Sullivan C, Zhao Q., Wang K., and Xu X. Body size distribution in a death
1101 assemblage of a colossal hadrosaurid from the Upper Cretaceous of Zhucheng, Shandong
1102 Province, China. In: Eberth D.A. and Evans D.C. (eds.). *Hadrosaurs*. Indiana University Press,
1103 Bloomington. pp. 524–531.
1104
1105 Hurlburt G. 1999. Comparison of body mass estimation techniques, using recent reptiles and the
1106 pelycosaur *Edaphosaurus boanerges*. *Journal of Vertebrate Paleontology* 19: 338-350.
1107
1108 Hurum J.H. and Sabath K. 2003. Giant theropod dinosaurs from Asia and North America: skulls
1109 of *Tarbosaurus bataar* and *Tyrannosaurus rex* compared. *Acta Palaeontologia Polonica* 48:161-
1110 190.
1111
1112 Hutchinson J.R., Anderson F.C., Blemker, S.S. and Delp S.L. 2005 Analysis of hind limb muscle
1113 moment arms in Tyrannosaurus rex using a three-dimensional musculoskeletal computer model:
1114 implications for stance, gait and speed. *Paleobiology* 31: 676 – 701
1115
1116 Hutchinson J.R., Bates K.T., Molnar J., Allen V. and Makovicky P.J. 2011. A computational
1117 analysis of limb and body dimensions in *Tyrannosaurus rex* with implications for locomotion,
1118 ontogeny, and growth. *PLoS One* 6(10): e26037. doi:10.1371/journal.pone.0026037.
1119
1120 Hutchinson J.R., Ng-Thow-Hing V. and Anderson F.C. 2007. A 3D interactive method for
1121 estimating body segmental parameters in animals: Application to the turning and running
1122 performance of *Tyrannosaurus rex*. *Journal of Theoretical Biology* 246: 660-680.
1123
1124 Huwaldt J.A. 2010. Plot Digitizer. http://plotdigitizer.sourceforge.net. Accessed August 19, 2011.
1125
1126 Irschick D.J. and Garland Jr, T. 2001. Integrating function and ecology in studies of adaptation:
1127 investigations of locomotor capacity as a model system. *Annual Review of Ecology and*
1128 *Systematics*. pp.367-396.
1129
1130 Jerison H.J. 1973. *Evolution of the brain and intelligence.* Academic Press. New York.

PeerJ Preprints | https://doi.org/10.7287/peerj.preprints.27021v1 | CC BY 4.0 Open Access | rec: 4 Jul 2018, publ: 4 Jul 2018

Läng E., Boudad L., Maio L. Samankassou E., Tabouelle J., Tong H., and Cavin L. 2013. Unbalanced food web in a Late Cretaceous dinosaur assemblage. *Palaeogeography, Palaeoclimatology, Palaeoecology* 381-382: 26-32.

Lauder, G. V. 1996. The argument from design. In: Rose M.R. and Lauder G.V. (eds.), *Adaptation.* Academic Press. San Diego. pp. 187–220.

Lauder G.V. and Reilly S.M. 1996. The mechanistic basis of behavioral evolution: Comparative analysis of muscoskeletal function. In: Martins (ed.), *Phylogenies and the Comparative Method in Animal Behavior*. Oxford University Press. Oxford. pp. 105–137.

Lehman T.M. and Coulson A.B. 2002. A juvenile specimen of the sauropod *Alamosaurus sanjuanensis* from the Upper Cretaceous of Big Bend National Park, Texas. *Journal of Palaeontology*. 7:156-172.

Li D., Norell M.A., Gao K.-Q., Smith N.D., and Makovicky P.J. 2009. A longirostrine tyrannosauroid from the Early Cretaceous of China. *Proceedings of the Royal Society of London , Series B* 277: 183-190.

Loewen M.A. 2009. Variation in the Late Jurassic theropod dinosaur *Allosaurus*: ontogenetic, functional, and taxonomic implications. Doctoral Thesis. The University of Utah.

Lü J., Yi L., Brusatte S.L., Yang L., Li H. and Chen L. 2014. A new clade of Asian Late Cretaceous long-snouted tyrannosaurids. *Nature Communications* 5: 3788

Madsen, J.H. Jr. 1976. *Allosaurus fragilis*: a revised osteology. *Bulletin 109, Utah Geological Survey.* 163 pp.

Maidment S.C.R., Bates K.T., Falkingham P.L., VanBuren C., Arbour V. and Barrett P.M. 2014. Locomotion in ornithischian dinosaurs: an assessment using three-dimensional computational modelling**.** *Biological Reviews* 89: 588-617.

Mallison, H. 2007. *Virtual Dinosaurs - Developing Computer Aided Design and Computer Aided Engineering Modeling Methods for Vertebrate Paleontology*. Doctoral Thesis. Eberhard-Karls-Universität, Tübingen, Germany. http://tobias-lib.ub.uni-tuebin- gen.de/volltexte/2007/2868/

Mallison H. 2010. The digital *Plateosaurus* I: body mass, mass distribution and posture assessed using CAD and CAE on a digitally mounted complete skeleton. *Palaeontologia Electronica* 13(2) 8A: 26p.

Mallison H. 2014. Osteoderm distribution has low impact on the centre of mass of stegosaurs. *Fossil Record* 17:33-39.

Mallison H., Pittman M. and Schwarz D. 2015. Using crocodilian tails as models for dinosaur tails. *PeerJ PrePrints* https://dx.doi.org/10.7287/peerj.preprints.1339v1

PeerJ Preprints | https://doi.org/10.7287/peerj.preprints.27021v1 | CC BY 4.0 Open Access | rec: 4 Jul 2018, publ: 4 Jul 2018

PeerJ Preprints NOT PEER-REVIEWED

Matthew W.D. and Brown B. 1923. Preliminary notices of skeletons and skulls of Deinodontidae from the Cretaceous of Alberta. *American Museum Novitates* 89: 1-10.

Mazzetta G.V., Christiansen P., and Fariña R.A. 2004. Giants and bizarres: body size of some southern South American Cretaceous dinosaurs. *Historical Biology* 2004: 1-13.

McGowen A.J. and Dyke G.J. 2009. A surfeit of theropods in the Moroccan Late Cretaceous? Comparing diversity estimates from field data and fossil shops. *Geology* 37: 843-846.

Moen D.S., Irschick D.J., and Wiens J.J. 2013. Evolutionary conservatism and convergence both lead to striking similarity in ecology, morphology and performance across continents in frogs. *Proceedings of the Royal Society B* 280: 20132156.

Moen D.S., Morlon H., and Wiens J.J. 2016. Testing convergence versus history: convergence dominates phenotypic evolution for over 150 million years in frogs. *Systematic Biology* 65: 146-160.

Motani R. 2001. Estimating body mass from silhouettes: testing the assumption of elliptical body cross-sections. *Paleobiology* 27: 735-750.

Orme D., Freckleton R., Thomas G., Petzoldt T., Fritz S., Isaac N., and Pearse W. 2013. caper: Comparative Analyses of Phylogenetics and Evolution in R. R package version 0.5.2. http://CRAN.R-project.org/package=caper

Osborn H.F. 1917. Skeletal adaptations of *Ornitholestes*, *Struthiomimus*, *Tyrannosaurus*. *Bulletin of the American Museum of Natural History* 35: 733-771.

Packard G.C., Boardman T.J., and Birchard G.F. 2009. Allometric equations for predicting body mass of dinosaurs. *Journal of Zoology* 279: 1-9.

Patel A. and M. Braae M. Rapid turning at high-speed: Inspirations from the cheetah's tail. *2013 IEEE/RSJ International Conference on Intelligent Robots and Systems*, Tokyo. pp. 5506-5511.

Patel A., Boje E., Fisher C., Louis L., and Lane E. 2016. Quasi-steady state aerodynamics of the cheetah tail. *Biology Open* 15;5(8):1072-6.

Paul G.S. 2010. *The Princeton Field Guide to Dinosaurs*. Princeton University Press. Princeton.

Paul G.S. 1988. *Predatory Dinosaurs of the World. A Complete Illustrated Guide*. Simon & Schuster. New York.

Peirce B.A.M. 1837. *An Elementary Treatise on Plane and Solid Geometry*. James Munroe and Company. Boston.

PeerJ Preprints | https://doi.org/10.7287/peerj.preprints.27021v1 | CC BY 4.0 Open Access | rec: 4 Jul 2018, publ: 4 Jul 2018

1222 Persons W.S. IV and Currie P.J. 2011. The tail of *Tyrannosaurus*: reassessing the size and
1223 locomotive importance of the M. caudofemoralis in non-avian theropods. *Anatomical Record*
1224 294: 119-131.
1225
1226 Peterson M.D., Alvar B.A. and Rhea M.R. 2006. The contribution of muscle force to explosive
1227 movement among young collegiate athletes. *Journal of Strength and Conditioning Research* 20:
1228 867-873.
1229
1230 Rankin J.W., Rubenson J. and Hutchinson J.R. 2016 Inferring muscle functional roles of the
1231 ostrich pelvic limb during walking and running using computer optimization. *Journal of the*
1232 *Royal Society Interface* 13: 20160035.
1233
1234 Rayfield, E.J. 2004. Cranial mechanics and feeding in *Tyrannosaurus rex*. *Proceedings of the*
1235 *Royal Society of London, Series B* 271: 1451–1459.
1236
1237 Revell L.J. 2010. Phylogenetic signal and linear regression on species data. *Methods in Ecology*
1238 *and Evolution* 1: 319-329.
1239
1240 Rosin P.L. 2000. Fitting superellipses. *IEEE Transactions on Pattern Analysis and Machine*
1241 *Intelligence* 22: 726-732.
1242
1243 Russell D.A. 1970. Tyrannosaurs from the Late Cretaceous of western Canada. *National*
1244 *Museum of Natural Sciences Publications in Paleontology* 1: 1-34.
1245
1246 Russell D.A. and Paesler M.A. 2003. Environments of Mid-Cretaceous Saharan dinosaurs.
1247 *Cretaceous Research* 24: 569–588.
1248
1249 Sellke T., Bayarri M.J., and Berger J.O. 2001 Calibration of *p* values for testing precise null
1250 hypotheses. *The American Statistician* 55: 62–71.
1251
1252 Sereno P.C., Tan L., Brusatte S.L., Kriegstein H.J., Zhao X. and Cloward K. 2009.
1253 Tyrannosaurid skeletal design first evolved at small body size. *Science*. 326: 418-422.
1254
1255 Smaers J.B. 2014. evomap: R package for the evolutionary mapping of continuous traits.
1256 Available at Github: https://github.com/JeroenSmaers/evomap.
1257
1258 Smaers J.B. and Rohlf F.J. 2016. Testing species' deviation from allometric predictions using the
1259 phylogenetic regression. *Evolution* 70: 1145-1149.
1260
1261 Snively E. 2012. Rigid body mechanics of prey capture in large carnivorous dinosaurs. M.Sc.
1262 Thesis. Ohio University.
1263
1264 Snively E. and Russell A.P. 2007a. Functional variation of neck muscles and their relation to
1265 feeding style in Tyrannosauridae and other large theropods. *Anatomical Record* 290: 934-957
1266

PeerJ Preprints | https://doi.org/10.7287/peerj.preprints.27021v1 | CC BY 4.0 Open Access | rec: 4 Jul 2018, publ: 4 Jul 2018

1267 Snively E. and Russell A.P. 2007b. Craniocervical feeding dynamics of *Tyrannosaurus rex*.
1268 *Paleobiology* 33: 610-638.
1269
1270 Snively E. and Russell A.P. 2003. Kinematic model of tyrannosaurid (Dinosauria: Theropoda)
1271 arctometatarsus function. *Journal of Morphology* 255: 215-227.
1272
1273 Snively, E., Henderson, D.M. and Phillips, D.S. 2006. Fused and vaulted nasals of tyrannosaurid
1274 dinosaurs: implications for cranial strength and feeding mechanics. *Acta Palaeontia Polonica* 51:
1275 435-454.
1276
1277 Snively E., Henderson D.M., Wick E., Sokup R., Roth P., and Dupor M. 2015. Ceratopsian
1278 dinosaurs could turn more quickly and iguanodontians comparably to contemporaneous large
1279 theropods. *Journal of Vertebrate Paleontology* 35:216A.
1280
1281 Stoinski S., Suthau T. and Gunga H.C. 2011. Reconstructing body volume and surface area of
1282 dinosaurs using laser scanning and photogrammetry. In: Klein N., Remes K., Gee C.T. and
1283 Sander P.M. (eds.). *Biology of the Sauropod Dinosaurs: Understanding the Life of Giants*.
1284 Indiana University Press. Bloomington. pp. 94-104.
1285
1286 Sullivan, R.M., and Lucas, S.G. 2006. The Kirtlandian land-vertebrate "age" – faunal
1287 composition, temporal position and biostratigraphic correlation in the nonmarine Upper
1288 Cretaceous of western North America. *New Mexico Museum of Natural History and Science,*
1289 *Bulletin* 35:7-29.
1290
1291 Symonds M.R.E. and Blomberg S.P. 2014. A primer on phylogenetic generalised least squares
1292 (PGLS). In: Garamszegi L.Z. (ed.). *Modern Phylogenetic Comparative Methods and Their*
1293 *Application in Evolutionary Biology: Concepts and Practice* Springer. Berlin. pp 105-130.
1294
1295 Taylor M.P. 2009. A re-evaluation of *Brachiosaurus altithorax* Riggs 1903 (Dinosauria,
1296 Sauropoda) and its generic separation from *Giraffatitan brancai* (Janensch 1914). *Journal of*
1297 *Vertebrate Paleontology* 29: 787-806.
1298
1299 Therrien F. and Henderson D.M. 2007. My theropod is bigger than yours… or not: estimating
1300 body size from skull length in theropods. *Journal of Vertebrate Paleontology* 27: 108-115.
1301
1302 Thomas K., French D. and Hayes P.R. 2009. The effect of two plyometric training techniques on
1303 muscular power and agility in youth soccer players. *Journal of Strength and Conditioning*
1304 *Research* 23: 332-335.
1305
1306 Tinius A., Russell A.P., Jamniczky H.A., and Anderson J.S. 2018. What is bred in the bone:
1307 Ecomorphological associations of pelvic girdle form in greater Antillean *Anolis* lizards. *Journal*
1308 *of Morphology* 2018;00: 1-15.
1309
1310 Trinkaus E., Churchill S.E., Villemeur I., Riley K.G., Heller J.A. and Ruff C.B. 1991.
1311 Robusticity versus shape: the functional interpretation of Neandertal appendicular morphology.
1312 *Journal of the Anthropological Society of Nippon* 99: 257–278.

PeerJ Preprints | https://doi.org/10.7287/peerj.preprints.27021v1 | CC BY 4.0 Open Access | rec: 4 Jul 2018, publ: 4 Jul 2018

PeerJ Preprints NOT PEER-REVIEWED

Varricchio D.J. 2001. Gut contents from a Cretaceous tyrannosaurid: implications for theropod dinosaur digestive tracts. *Journal of Paleontology* 75: 401-406.

Walker A.D. 1964. Triassic reptiles from the Elgin area: *Ornithosuchus* and the origin of carnosaurs. *Philosophical Transactions of the Royal Society of London* 248: 53-134.

Wegweiser M., Breithaupt B., and Chapman R. 2004. Attack behavior of tyrannosaurid dinosaur(s): Cretaceous crime scenes, really old evidence, and "smoking guns." *Journal of Vertebrate Paleontology* 24(Supplement 3), 127A.

Weiss T., Kreitinger J., Wilde H., Wiora C., Steege M., Dalleck L. and Janot J. 2010. Effect of functional resistance training on muscular fitness outcomes in young adults. *Journal of Exercise Science and Fitness* 2: 113-122.

Wilson A.M., Lowe J.C., Roskilly K., Hudson P.E., Golabek K.A. and McNutt J.W. 2013. Locomotion dynamics of hunting in wild cheetahs. *Nature* 498: 185-189.

Witmer L.M. and Ridgely R.C. 2008. The paranasal air sinuses of predatory and armored dinosaurs (Archosauria: Theropoda and Ankylosauria) and their contribution to cephalic structure. *Anatomical Record* 291: 1362-1388.

Young W.B., James R. and Montgomery I. 2002. Is muscle power related to running speed with changes in direction? *Journal of Sports Medicine and Physical Fitness* 42: 282-288.

PeerJ Preprints | https://doi.org/10.7287/peerj.preprints.27021v1 | CC BY 4.0 Open Access | rec: 4 Jul 2018, publ: 4 Jul 2018

1338 Table 1. Muscles originating from the ilium and tail of theropod dinosaurs (Carrano and
1339 Hutchinson 2002, Mallison et al. 2015) and their utility for yaw (turning the body laterally).
1340 Although few muscles pivot the body directly over the stance leg (Mm. caudofemoralis brevis et
1341 longus, M. ilio-ischiocaudalis), all large ilium-based muscles are potentially involved with
1342 turning by acceleration of the body on the outside of the turn, stabilization of the hip joint, or
1343 conservation of angular momentum by swinging the tail.
1344

Muscle	Action	Effect on turning (yaw)
Ilium origin		
M. iliotibialis 1	Knee extension, hip flexion	Greater acceleration outside turn, stabilization inside turn
M. iliotibialis 2	Knee extension, hip flexion	Greater acceleration outside turn, stabilization inside turn
M. iliotibialis 3	Knee extension	Greater acceleration outside turn, stabilization inside turn
M. iliotrochantericus caudalis	Hip abduction	Joint stabilization
M. iliofemoralis externus	Hip abduction	Joint stabilization
M. iliofemoralis internus	Hip abduction	Joint stabilization
M. caudofemorais brevis	Femoral retraction, direct yaw of body, pitch of body	Yaw with unilateral contraction, contralateral braking
Tail origin		
M. caudofemoralis longus	Femoral retraction, direct yaw of body, pitch of body	Yaw with unilateral contraction, Ipsilateral yaw by conservation of angular momentum, contralateral braking
Ilium origin, tail insertion		
M. ilio-ischiocaudalis (dorsal)	Tail lateral and dorsal flexion	Ipsilateral yaw by conservation of angular momentum, contralateral braking

PeerJ Preprints | https://doi.org/10.7287/peerj.preprints.27021v1 | CC BY 4.0 Open Access | rec: 4 Jul 2018, publ: 4 Jul 2018

PeerJ Preprints NOT PEER-REVIEWED

1345 Table 2. Theropod taxa, specimens, and data sources for calculations of mass, mass moment of
1346 inertia, and ilium area.
1347

Taxon	Specimen #	Lateral view	Dorsal view/ modified from	Ilium source
Dilophosaurus wetherelli	UCMP 37302	Paul 2010, Hartman 2015, Allen et al. 2013	Paul 2010†, Allen et al. 2013	Hartman 2015
Ceratosaurus nasicornis	USNM 4735	Paul 2010	Paul 2010	photo; Gilmore 1920
Basal tetanurae				
Eustreptospondylus oxoniensis	OUM J13558	Paul 2010	Paul 1988, Walker 1964	Walker 1964
Allosaurus fragilis	USNM 4734, UUVP 6000	Paul 2010, Paul 1988	Paul 2010	Paul 2010, Madsen 1976
Allosaurus jimmadseni (tail restored)	MOR 693	Bates et al. 2009	Paul 2010	photo; Loewen 2009
Acrocanthosaurus atokensis	NCSM 14345	Bates et al. 2010	Bates et al. 2010	photo, Bates et al. 2012 (restored)
Giganotosaurus carolinii	MUCPv-CH-1	Paul 2010, Hartman 2015	Paul 2010, Coria and Currie 2002 †	photo; Hartman 2015
Sinraptor hepingensis	ZDM 0024	Paul 2010	Paul 2010, Gao 1992	Gao 1992
Yangchuanosaurus shangyouensis	CV 00215	Paul 2010	Paul 2010	Dong et al. 1983
Tyrannosauroidea				
Raptorex kriegsteini (small juvenile *Tarbosaurus*)	LH PV18	Paul 2010	Sereno et al. 2010	Sereno et al. 2010
Tarbosaurus bataar (juvenile)	ZPAL MgD-I/3	Paul 1988, 2010	Paul 1988†	photo; Paul 1988
Tarbosaurus bataar (adult)	ZPAL MgD-I/4	Paul 2010	Hurum and Sabath 2003	photo
Tarbosaurus bataar (adult)	PIN 552-1	Paul 2010	Paul 1988†	Paul 1988, Maleev 1974
Tyrannosaurus rex (juvenile)	BMRP 2002.4.1	Paul 2010	Persons and Currie 2011	photo; Paul 2010
Tyrannosaurus rex (adult)	AMNH 5027, CM 9380	Paul 2010, Hartman 2004	Persons and Currie 2011	photo; Osborn 1917
Tyrannosaurus rex (adult)	FMNH PR 2081	Hartman 2004	Persons and Currie 2011	photo; Brochu 2003
Gorgosaurus libratus (adult)	AMNH 5458, NMC 2120	Paul 2010, 1988	Paul 1988	photo; Paul 2010
Gorgosaurus libratus (juvenile)	AMNH 5664	Paul 2010	Paul 1988	photo; Matthew and Brown 1923
Gorgosaurus libratus (juvenile)	TMP 91.36.500	Currie 2003, Hartman 2015	Paul 1988	photo; Currie 2003, Hartman 2015
Daspletosaurus torosus	CMN 8506	Paul 2010	Paul 1988, Russell 1970	Russell 1970

1348
1349 † = Different genus used for modified dorsal body outline.
1350 Institutional abbreviations: AMNH=American Museum of Natural History. BMRP=Burpee Museum (Rockford),
1351 Paleontology. CM=Carnegie Museum of Natural History. CMN=Canadian Museum of Nature. CV= Municipal
1352 Museum of Chunking. FMNH=Field Museum of Natural History. LH PV=Long Hao Institute of Geology and

PeerJ Preprints | https://doi.org/10.7287/peerj.preprints.27021v1 | CC BY 4.0 Open Access | rec: 4 Jul 2018, publ: 4 Jul 2018

PeerJ Preprints NOT PEER-REVIEWED

Paleontology. MOR=Museum of the Rockies. MUCPv=Museo de la Universidad Nacional del Comahue, El Chocón collection. NCSM=North Carolina State Museum. NMC= National Museum of Canada. OUM=Oxford University Museum. PIN=Paleontological Institute, Russian Academy of Sciences. TMP=Royal Tyrrell Museum of Palaeontology; UCMP=University of California Museum of Paleontology. USNM= United States National Museum. UUVP=University of Utah Vertebrate Paleontology. ZDM= Zigong Dinosaur Museum. ZPAL=Paleobiological Institute of the Polish Academy of Sciences.

PeerJ Preprints | https://doi.org/10.7287/peerj.preprints.27021v1 | CC BY 4.0 Open Access | rec: 4 Jul 2018, publ: 4 Jul 2018

PeerJ Preprints NOT PEER-REVIEWED

Table 3. Ilium area, mass properties, and relative agility of theropod dinosaurs. Mass properties are "best estimate" values, assuming superellipse body cross sections with exponent k=2.3 (compared with k=2 for an ellipse). This cross section is common for terrestrial vertebrates, and has 4.7% greater area than an ellipse of the same radii. Differing exponents, specific tension coefficients for absolute muscle force, and relative moment arms (scaled as body mass$^{1/3}$) do not change relative agilities of tyrannosaurids and large non-tyrannosaurids predatory theropods. $Agility_{force}$ is an estimate of relative maneuverability based on a human athletic standard that finds turning ability is highly correlated with leg muscle force/body mass ratio. $Agility_{moment}$ enables comparison of turning ability by incorporating scaled moment arms for estimating relative torques. As a first approximation, $Agility_{moment}$ assumes similar scaling of moment arms across all taxa.

Table 3 is on the next page.

PeerJ Preprints | https://doi.org/10.7287/peerj.preprints.27021v1 | CC BY 4.0 Open Access | rec: 4 Jul 2018, publ: 4 Jul 2018

PeerJ Preprints NOT PEER-REVIEWED

	Ilium area	**Total Mass**		**Mass moments of inertia**			***Agility*** ***force*** axial body	***Agility*** ***moment*** axial body	***Agility*** ***force*** body+leg	***Agility*** ***moment*** body+leg
	A (cm^2)	kg	log10	$I_{y\ body}$ ($kgxm^2$)	$I_{y\ leg}$ ($kgxm^2$)	$I_{y\ body+leg}$ ($kgxm^2$)	A/I	$\tau_{relative}/I$	A/I	$\tau_{relative}/I$
Taxon										
Dilophosaurus wetherelli	380.16	372.07	2.571	213	0.279	218	1.78	2.57	1.75	2.51
Ceratosaurus nasicornis	903.83	678.26	2.831	546	1.093	559	1.60	2.21891	1.57	2.61
Eustreptospondylus oxoniensis	280	206.26	2.314	70.45	0.098	73.26	3.97	4.70	3.82	4.52
Allosaurus fragilis	1131.5	1512.10	3.180	2303.25	2.405	2344.62	0.49	1.13	0.48	1.11
Allosaurus fragilis	1228.06	1683.33	3.226	2036.81	2.121	2078.55	0.60	1.43	0.59	1.41
Acrocanthosaurus atokensis	2551.25	5474.1	3.738	14979	19.718	15377.24	0.17	0.60	0.17	0.58
Giganotosaurus carolinii	3540.64	6907.6	3.839	35821	23.731	26593.36	0.10	0.511	0.13	0.507
Sinraptor hepingensis	1268.9	2373.5	3.430	3530.7	4.929	3740.32	0.343	0.93	0.339	0.91
Yangchuanosaurus shangyouensis	992.4	2176.4	3.173	2836.7	3.365	1672.88	0.61	1.36	0.59	1.31
Raptorex kriegsteini	179.7	47.07	1.673	4.65	0.0205	4.68	43.96	31.74	43.60	31.49
Tarbosaurus bataar (juvenile)	1455.2	727.45	2.861	535	1.437	548	2.72	2.39	2.65	4.77
Tarbosaurus bataar (adult)	2800	2249.1	3.352	3069.9	5.586	3126.17	0.912	2.39	0.905	2.37
Tarbosaurus bataar (adult)	2977	2816.3	3.450	4486	10.049	4515.1	0.664	1.87	0.659	1.86
Tyrannosaurus rex (juvenile)	1107.41	660.23	2.820	344.83	0.683	347	3.21	5.59	3.19	5.56
Tyrannosaurus rex (adult)	4786.49	6986.6	3.844	18175	34.067	18276.08	0.263	1.01	0.262	1.00
Tyrannosaurus rex (adult)	6661.8	9130.87	3.963	28847	51.205	29297	0.231	0.97	0.227	0.95
Gorgosaurus libratus (adult)	2358	2427.3	3.385	3219	9.79	3312	0.73	1.97	0.70	1.67
Gorgosaurus libratus (juvenile)	1040.56	687.7	2.837	402	1.087	420.14	2.59	4.56	2.48	4.37
Gorgosaurus libratus (juvenile)	1060.93	496.1	2.70	251.95	0.660	265.29	4.21	6.67	4.00	6.33
Daspletosaurus torosus	3209.77	3084.8	3.489	5338	9.665	5586	0.60	1.75	0.58	1.67

PeerJ Preprints | https://doi.org/10.7287/peerj.preprints.27021v1 | CC BY 4.0 Open Access | rec: 4 Jul 2018, publ: 4 Jul 2018

PeerJ Preprints NOT PEER-REVIEWED

Table 4. Centers of mass (COM) and rotation axes for large theropod dinosaurs. Axial body: The x value is the position (m) from the anterior tip of the rostrum (where x=0), and y value is the distance (m) from the ventral point of the body (y=0). The z position is 0, at the midline of the body, because the body is modeled as symmetrical. Swing leg: This is the positive z coordinate position (in m) of the leg relative to that of the axial body's COM. Axial body+swing leg: The z coordinate positon (m) of the collective COM of the body and swing leg. The value is small because the leg's mass is much less than that of the axial body.

	Axial body COM (z=0)		Swing leg rotation axis		Axial body +swing leg rotation axis	
Taxon	x	y	x	z	x	z
Dilophosaurus wetherelli	2.33	0.42	2.61	0.17	2.36	0.02
Ceratosaurus nasicornis	2.66	0.50	3.07	0.15	2.70	0.01
Eustreptospondylus oxoniensis	1.46	0.33	1.84	0.10	1.51	0.01
Allosaurus fragilis	2.72	0.64	3.26	0.0.24	2.77	0.02
Allosaurus jimmadseni	2.64	0.79	3.20	0.23	2.69	0.02
Acrocanthosaurus atokensis	4.34	0.91	4.69	0.46	4.36	0.03
Giganotosaurus carolinii	4.54	1.33	5.10	0.44	4.57	0.03
Sinraptor hepingensis	3.12	0.86	3.57	0.15	3.16	0.01
Yangchuanosaurus shangyouensis	2.40	0.72	2.99	0.23	2.45	0.02
Tarbosaurus bataar (juvenile)/*Raptorex*	0.87	0.22	0.05	0.0073	0.88	0.007
Tarbosaurus bataar (juvenile)	1.93	0.54	2.33	0.15	1.98	0.02
Tarbosaurus bataar (ZPAL)	2.85	0.80	0.31	0.027	2.87	0.014
Tarbosaurus bataar (adult)	3.01	0.87	0.29	0.028	2.07	0.025
Tyrannosaurus rex (juvenile)	2.19	0.60	0.16	0.018	2.19	0.02
Tyrannosaurus rex (adult)	3.82	1.15	0.36	0.032	3.87	0.04
Tyrannosaurus rex (adult)	3.84	1.17	0.40	0.040	3.90	0.04
Gorgosaurus libratus (adult)	3.20	0.89	3.72	0.29	3.27	0.04
Gorgosaurus libratus (AMNH juvenile)	1.73	0.49	2.21	0.18	1.79	0.02
Gorgosaurus libratus (TMP juvenile)	2.03	0.52	2.51	0.13	2.10	0.02
Daspletosaurus torosus	3.35	1.16	3.93	0.25	3.43	0.05

PeerJ Preprints | https://doi.org/10.7287/peerj.preprints.27021v1 | CC BY 4.0 Open Access | rec: 4 Jul 2018, publ: 4 Jul 2018

PeerJ Preprints NOT PEER-REVIEWED

1384 Table 5. Variation of mass properties with different tail widths. The last three columns are percentages relative to the baseline values.
1385

Taxon	Specimen	mass: initial kg	mass: 1.4 tail kg	CM initial m from rostrum	CM 1.4 tail	I_y initial	I_y 1.4 tail	mass: % initial	CM: % initial	I_y: % initial
Tarbosaurus bataar	ZPAL MgD-I/4	2249	2367	2.68	2.97	3070	3578	105.2	110.8	116.5
Tyrannosaurus rex	AMNH 5027	6986	7458	3.82	4.01	18175	21395	106.7	105	117.7
Tyrannosaurus rex	FMNH PR 2081	9131	9657	3.79	4.24	28847	34742	105.1	111.9	120.4
Acrocanthosaurus atokensis	NCSM 14345	5603	6560	4.09	4.49	14978	22083	117.1	109.8	147.4
Allosaurus fragilis	USNM 4734	1356	1456	2.42	2.78	1662	1982	107.4	114.9	119.3
Yanchuanosaurus shangyouensis	CV 00215	1362	1441	2.64	2.95	1613	1905	105.8	111.7	118.1
Sinraptor hepingensis	ZDM 0024	2428	2588	3.12	3.37	3694	4374	106.6	108	118.4

PeerJ Preprints | https://doi.org/10.7287/peerj.preprints.27021v1 | CC BY 4.0 Open Access | rec: 4 Jul 2018, publ: 4 Jul 2018

PeerJ Preprints NOT PEER-REVIEWED

1387 Table 6. Comparisons of $Agility_{force}$ and $Agility_{moment}$ between groups of theropods turning their
1388 bodies, with both legs planted on the ground. Among groups compares adult+juvenile
1389 tyrannosaurids with non-tyrannosaurid theropods. Tyrannosaurs vs. Juveniles compares adult
1390 and juvenile tyrannosaurid specimens, and Tyrannosaurs vs. Other Theropods compares adults
1391 alone. Tyrannosaurids have significantly greater agility values than other theropods regardless of
1392 grouping, but juvenile and adult tyrannosaurids share an allometric continuum.
1393

Groupings	$Agility_{force}$		$Agility_{moment}$	
	F	*P*	*F*	*P*
Among Groups	15.843	0.0002	8.8688	0.0026
Tyrannosaurs vs. Juveniles	0.6670	0.4216	0.2261	0.6409
Tyrannosaurs vs. Other Theropods	26.067	0.0001	15.9674	0.0010

1394

PeerJ Preprints | https://doi.org/10.7287/peerj.preprints.27021v1 | CC BY 4.0 Open Access | rec: 4 Jul 2018, publ: 4 Jul 2018

PeerJ Preprints NOT PEER-REVIEWED

1395 Table 7. Comparisons of $Agility_{force}$ and $Agility_{moment}$ between groups of theropods turning while
1396 pivoting on one foot ("en pointe"). Among groups compares adult+juvenile tyrannosaurids with
1397 non-tyrannosaurid theropods. Tyrannosaurs vs. Juveniles compares adult and juvenile
1398 tyrannosaurid specimens, and Tyrannosaurs vs. Other Theropods compares adults alone.
1399 Tyrannosaurids have significantly greater agility values than other theropods regardless of
1400 grouping, but juvenile and adult tyrannosaurids share an allometric continuum.
1401

Groupings	$Agility_{force}$		$Agility_{moment}$	
	F	*P*	*F*	*P*
Among Groups	11.9197	0.0007	11.9537	0.0007
Tyrannosaurs vs. Juveniles	0.2970	0.5933	0.2814	0.6031
Tyrannosaurs vs. Other Theropods	21.441	0.0003	21.5640	0.0003

1402

PeerJ Preprints | https://doi.org/10.7287/peerj.preprints.27021v1 | CC BY 4.0 Open Access | rec: 4 Jul 2018, publ: 4 Jul 2018

Figure 1.

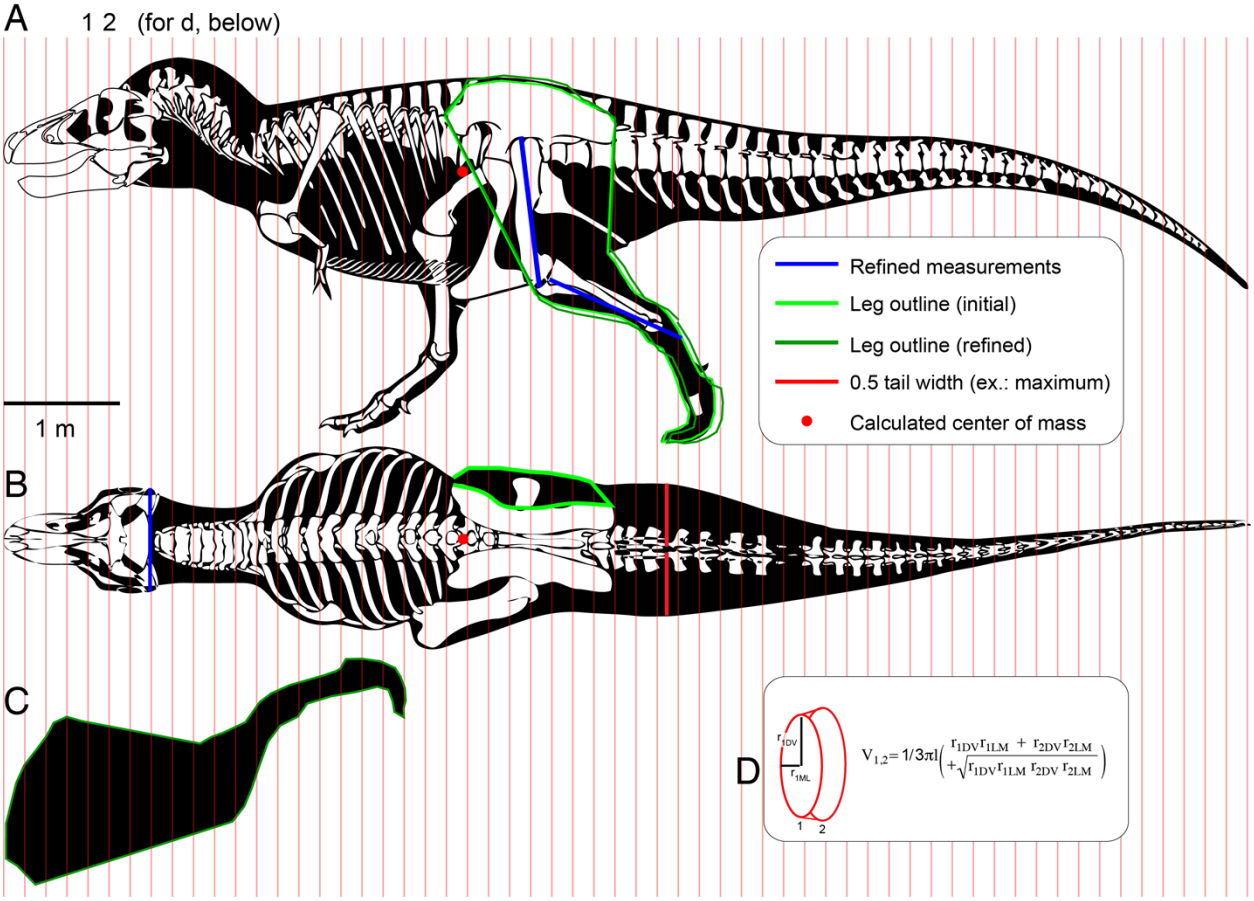

Figure 1. Methods for digitizing body outlines and calculating mass properties, for "maximum tail width" estimate for *Tyrannosaurus rex*. Reconstructions of *Tyrannosaurus rex* (Field Museum FMNH PR 2081) in lateral view (A: after Hartman 2011) and dorsal view (B: after Paul 2010) enable digitizing of dorsal, ventral, and lateral extrema where they cross the vertical red lines. The lateral view (A) is modified with the mouth nearly closed, and dorsal margin of the neck conservatively raised based on recent muscle reconstructions (Snively and Russell 2007a, b). The dorsal view is modified through measurement of the width of the cranium (blue line; Brochu 2003), and a tail width based on maxima found for *Alligator* (Mallison et al. 2015). The hind leg (A and C) is modified (dark green outlines) based on measurements in Brochu (2003), shown by blue lines in A. A red dot (A and B) specifies the center of mass of the axial body (minus the limbs) using this reconstruction. An equation for the volume of a given frustum of the body (D), between positions 1 and 2, assumes elliptical cross sections. Note that the head in the lateral view is tilted up to match the strict dorsal view of the skull in B, which is necessary for correct scaling. This reconstruction, with a particularly thick tail, yielded our highest mass

PeerJ Preprints | https://doi.org/10.7287/peerj.preprints.27021v1 | CC BY 4.0 Open Access | rec: 4 Jul 2018, publ: 4 Jul 2018

PeerJ Preprints NOT PEER-REVIEWED

estimate for this specimen at 9.7 tonnes, and the farthest posterior center of mass. The thinner-tailed reconstruction used in regressions had a mass of 9.1 tonnes, for consistency with reconstructions of other modeled taxa.

PeerJ Preprints | https://doi.org/10.7287/peerj.preprints.27021v1 | CC BY 4.0 Open Access | rec: 4 Jul 2018, publ: 4 Jul 2018

PeerJ Preprints NOT PEER-REVIEWED

Figure 2.

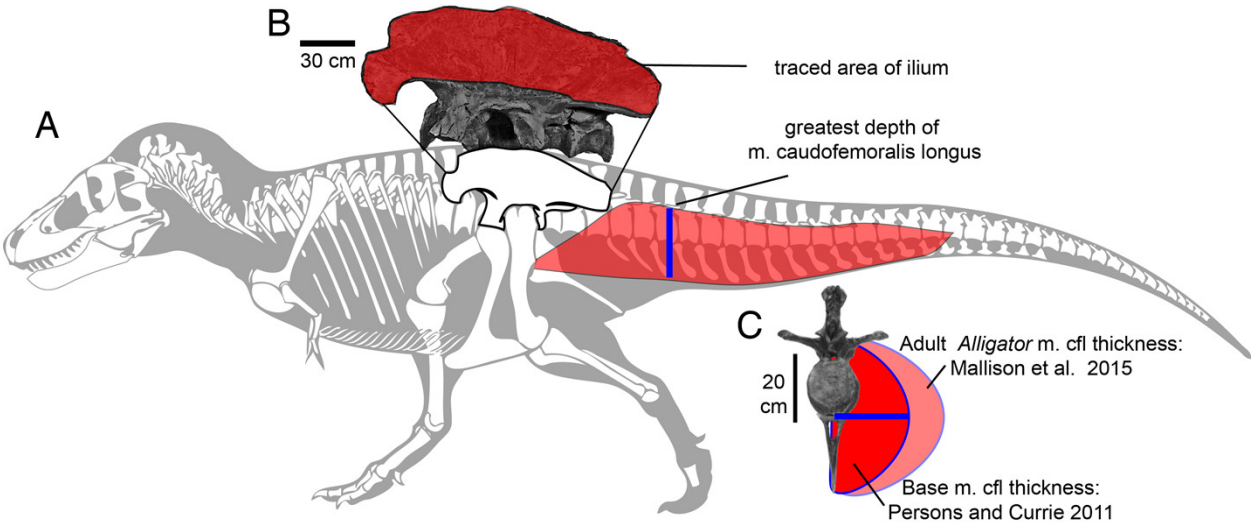

Figure 2. Methods for approximating attachment cross-sectional area of hind limb muscles, on lateral view (A) of a *Tyrannosaurus rex* skeleton (FMNH PR 2081; modified from Hartman 2011). The blue line shows the position of the greatest depth from the caudal ribs to the ventral tips of the chevrons, and greatest inferred width of the m. caudofemoralis longus. B. The inferred region of muscle attachment on the ilium (modified from Brochu 2003) is outlined in red, for scaled area measurement in ImageJ. C. The initial reconstructed radius (blue) of m. caufofemoralis longus (CFL) is 0.5 times the hypaxial depth of the tail (blue line in a), seen in anterior view of free caudal vertebra 3 and chevron 3. The maximum lateral extent of CFL is here based on cross-sections of adult *Alligator mississippiensis* (Mallison et al. 2015). Note that the chevron in c is modified to be 0.93 of its full length, because it slopes posteroventrally when properly articulated (Brochu 2003). Bone images in A and C are "cartoonized" in Adobe Photoshop to enhance edges.

PeerJ Preprints | https://doi.org/10.7287/peerj.preprints.27021v1 | CC BY 4.0 Open Access | rec: 4 Jul 2018, publ: 4 Jul 2018

PeerJ Preprints NOT PEER-REVIEWED

1447 Figure 3 (caption on next page).

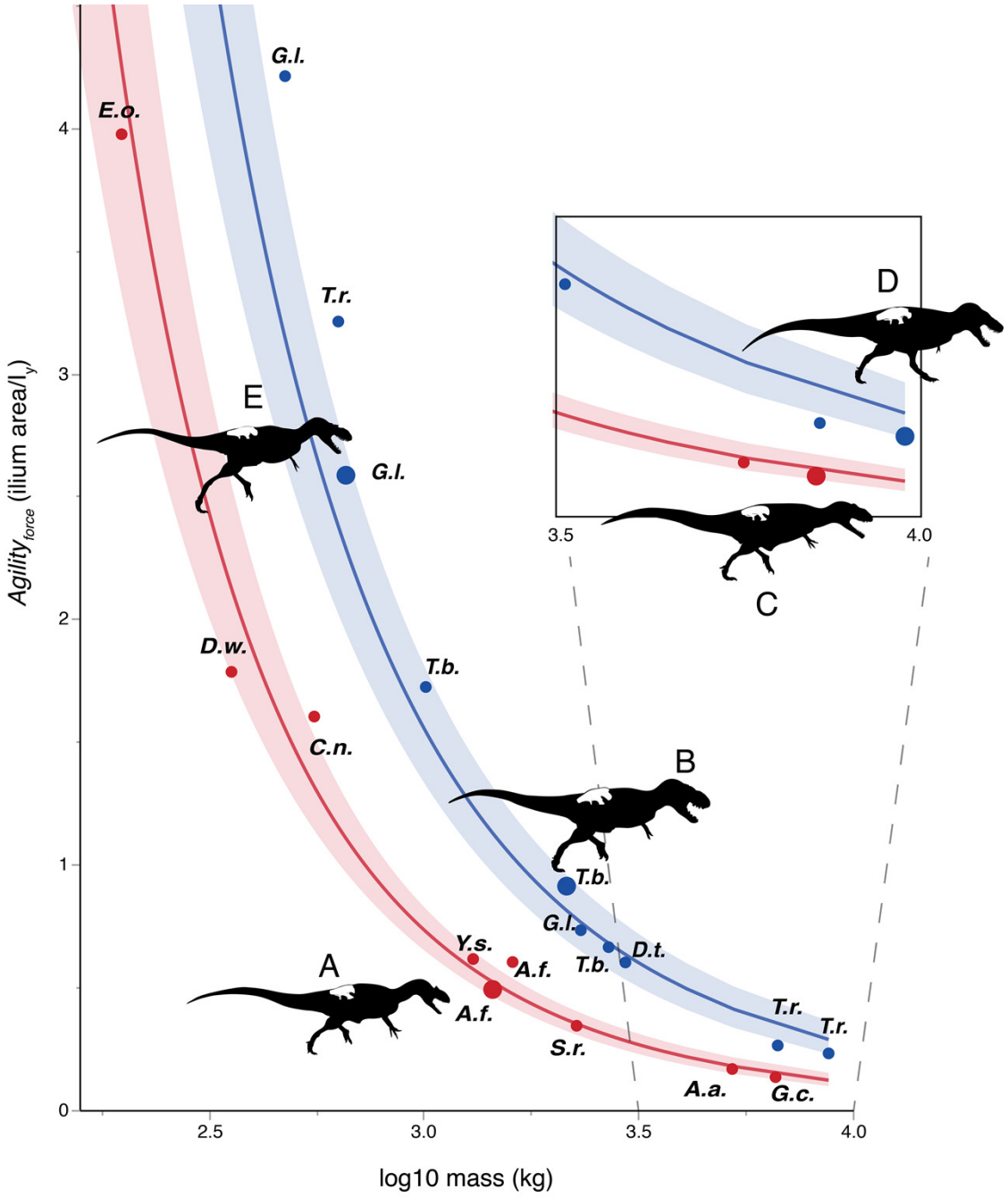

1448
1449
1450
1451
1452
1453
1454

PeerJ Preprints | https://doi.org/10.7287/peerj.preprints.27021v1 | CC BY 4.0 Open Access | rec: 4 Jul 2018, publ: 4 Jul 2018

Figure 3. Log-linear plot of body mass (x-axis) versus an agility index (y-axis) based on muscles originating from the ilium, with tyrannosauruids in blue and non-tyrannosaurids in red. 95% confidence intervals do not overlap. Larger circles show positions of depicted specimens. A. *Allosaurus fragilis*. B. *Tarbosaurus bataar*. C. *Giganotosaurus carolinii* (a shorter-headed reconstruction was used for regressions). D. *Tyrannosaurus rex*. E. *Gorgosaurus libratus* (juvenile). The *Tyrannosaurus rex* silhouette is modified after Hartman (2011); others are modified after Paul (1988, 2010). The inset enlarges results for theropods larger than 3 tonnes in mass. Note that the tyrannosaurids have 2-5 times the agility index magnitudes of other theropods of similar mass. Discrepancies between tyrannosaurids and non-tyrannosaurids are greater at smaller body sizes.

Abbreviations: *A.a.=Acrocanthosaurus*; A.f.=*Allosaurus*; *C.n.=Ceratosaurus*; *D.t.=Daspletosaurus*; *D.w.=Dilophosaurus*; *E.o.=Eustreptospondylus oxoniensis*; *G.c.=Giganotosaurus; G.l.=Gorgosaurus*; *S.h.=Sinraptor*; *T.b.=Tarbosaurus*; *T.r.=Tyrannosaurus*; *Y.s.=Yangchuanosaurus*.

PeerJ Preprints | https://doi.org/10.7287/peerj.preprints.27021v1 | CC BY 4.0 Open Access | rec: 4 Jul 2018, publ: 4 Jul 2018

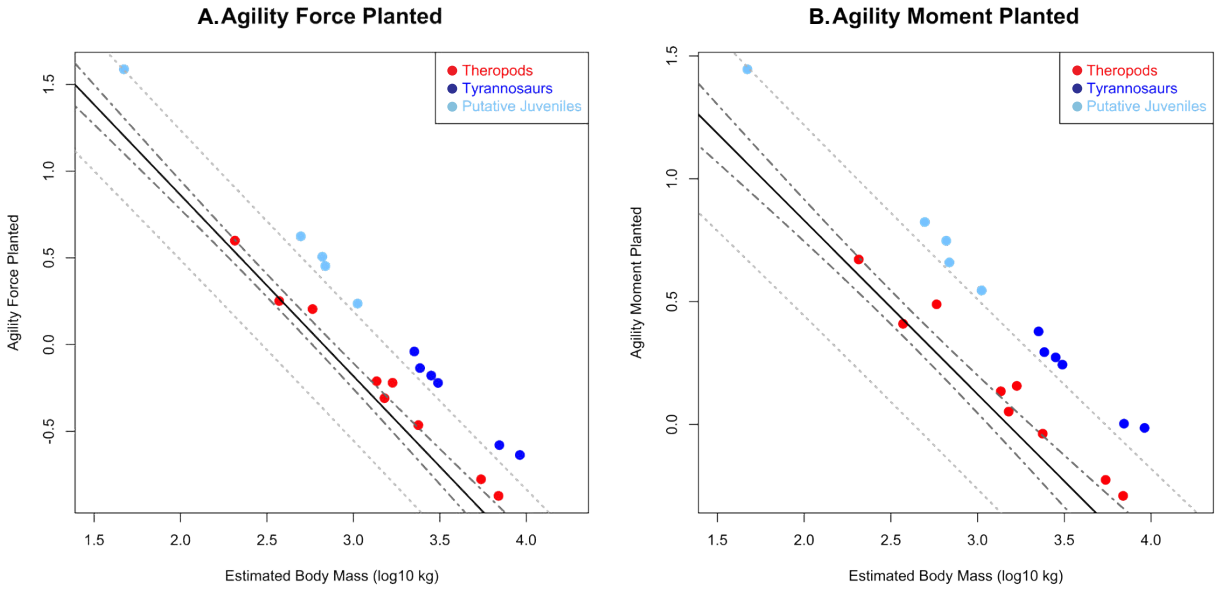

Figure 4. Phylogenetically generalized least squares regressions of (A) $Agility_{force}$ and (B) $Agility_{moment}$ for non-tyrannosaurid theropods (red), adult tyrannosaurids (dark blue), and putative juvenile tyrannosaurids (light blue), turning the body with both legs planted. Tyrannosaurids lie above or on the upper 95% confidence limit of the regression, indicating definitively greater agility than expected for theropods overall when pivoting the body alone. See Figure 1, and Supplementary Information figure and R script, for data point labels.

PeerJ Preprints | https://doi.org/10.7287/peerj.preprints.27021v1 | CC BY 4.0 Open Access | rec: 4 Jul 2018, publ: 4 Jul 2018

1483

1484

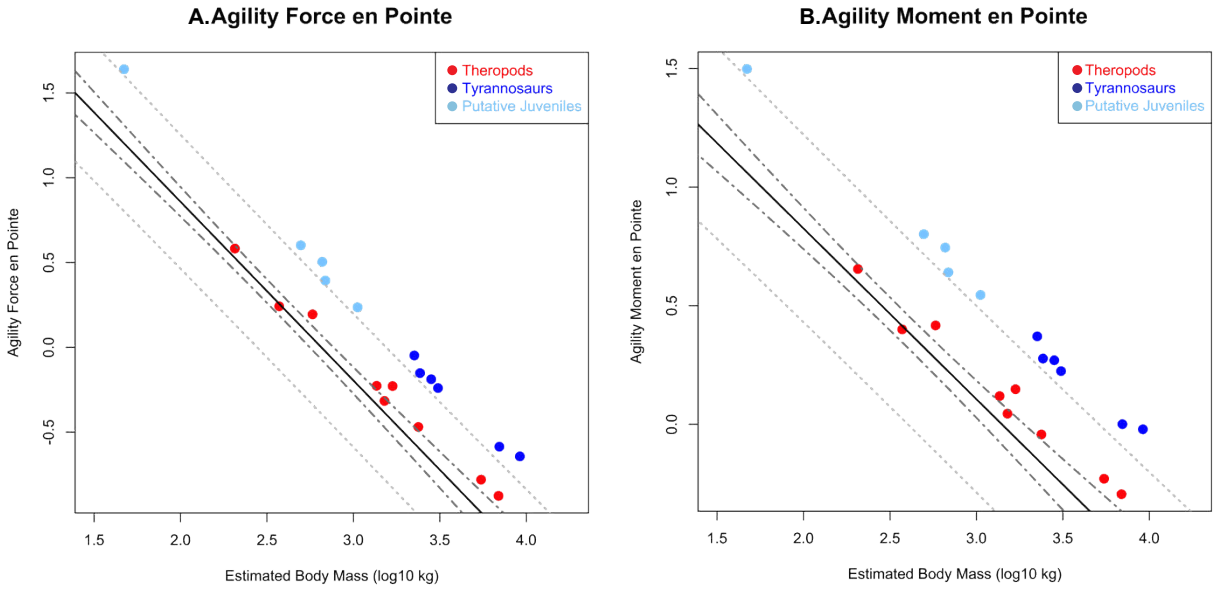

1485

1486 Figure 5. Phylogenetically generalized least squares regression of (A) $Agility_{force}$ and (B)
1487 $Agility_{moment}$ for non-tyrannosaurid theropods (red), adult tyrannosaurids (dark blue), and putative
1488 juvenile tyrannosaurids (light blue), when pivoting on one leg (en pointe). Tyrannosaurids lie
1489 above or on the upper 95% confidence limit of the regression, indicating definitively greater
1490 agility than expected for theropods when pursuing prey. See Figure 1, and the Supplementary
1491 Information figure and R script, for data point labels.

1492

PeerJ Preprints | https://doi.org/10.7287/peerj.preprints.27021v1 | CC BY 4.0 Open Access | rec: 4 Jul 2018, publ: 4 Jul 2018

Figure 6.

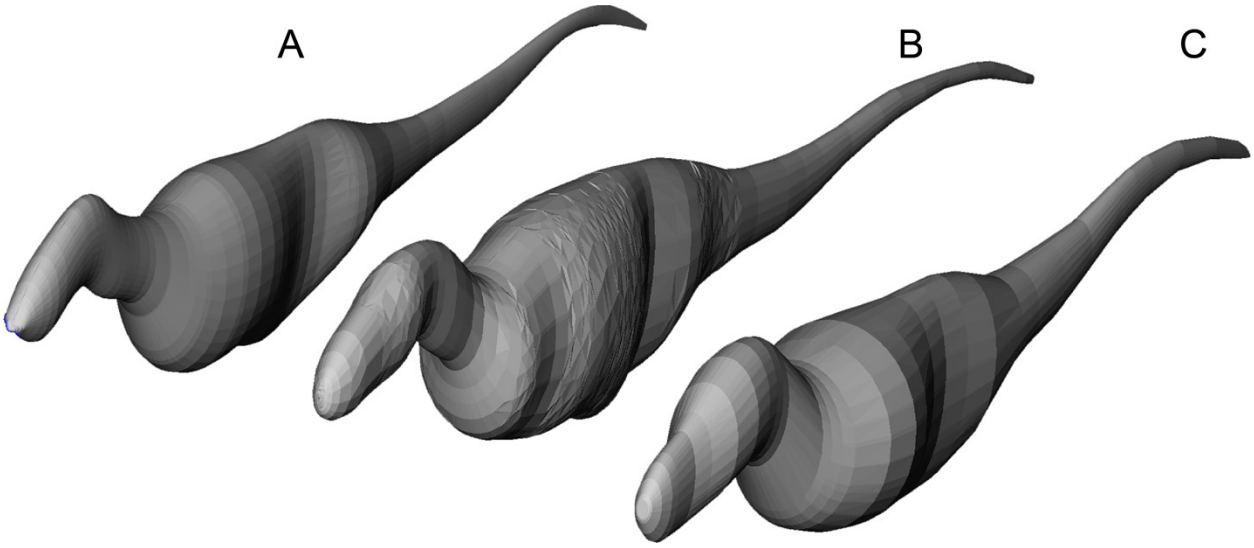

Figure 6. Axial body models (constructed in FreeCAD) of (A) *Yangchuanosaurus shangyouensis* (CV 00215), (B) *Sinraptor hepingensis* (ZDM 0024) and (C) *Tarbosaurus bataar* (ZPAL MgD-I/4) are within 0.5% of the volumes calculated by summing frusta volumes from equation 2. Three workers built different respective models, and congruence of results suggests low operator variation and high precision between the methods. The *Tarbosaurus* is lofted from fewer elliptical cross sections than the others, giving it a smoother appearance that nevertheless converges on the frustum results from many more cross-sections. Note that this is an exercise in cross-validation of volume estimates using uniform densities. Our mass property comparisons use frustum-based calculations that incorporate different densities for different regions of the body.

PeerJ Preprints | https://doi.org/10.7287/peerj.preprints.27021v1 | CC BY 4.0 Open Access | rec: 4 Jul 2018, publ: 4 Jul 2018